



Technische Universität
Wien



University of L'Aquila

Joint Master's Programme - MathMod Mathematical Modelling in Engineering: Theory, Numerics, Applications

Master of Science
Mathematical Modelling in Engineering:
Theory, Numerics, Applications

TECHNISCHE UNIVERSITÄT WIEN (TUW)

Laurea Magistrale
Mathematical Modelling

UNIVERSITY OF L'AQUILA (UAQ)

Master's Thesis

*Multiphase CFD Modelling & Simulation of Evaporation from
Porous Medium*

Supervisor

Ao.Univ.Prof. Dipl.-Ing Dr.techn. Michael

Harasel

Co-advisor

Projektass. Dr.techn. Bahram Hadaddi

Sisakht

Projektass. Dipl.-Ing. Thorsten Jonach

Candidate

Rohit Raj

Student ID (UAQ): 274465

Student ID (TUV): 12045331

Declaration of Authorship

I, Rohit RAJ, declare that this thesis titled, "*Multi-phase CFD Modelling and Simulation of Evaporation from Porous Media*" and the presented work are my own. I also confirm that:

- I performed the associated research and wrote the thesis on my own.
- I have quoted the research work of others in the bibliography.
- I have acknowledged all the primary sources of help.
- This work is original and has not been submitted elsewhere for any examination, nor is it under consideration.

Signed:

Date:

TECHNISCHE UNIVERSITÄT WIEN

Abstract

Research Division: Thermal Process Engineering and Simulation

Research Group: Computational Fluid Dynamics (CFD)

Institute of Chemical, Environmental and Bioscience Engineering

Master of Science

Multiphase CFD Modelling and Simulation of Evaporation from Porous Media

by Rohit RAJ

Evaporation of liquids from porous media appears ubiquitously in nature and technical applications. Evaporation from the soil, drying of foods, drying of building materials and baking are some crucial examples. In general, it is a coupled process where the evaporation occurs at the interface of the porous media, which is exposed to a free flow region. In the coupled process, various physical effects occur simultaneously. The key processes influencing evaporation are the transport of liquids through porous media, pore structure, heat transfer and coupling with the boundary. *Computational Fluid Dynamics (CFD)* methods can be employed to improve the understanding of the effects of evaporation from porous fluid reservoirs. To develop mathematical models to study such effects, suitable coupling methods are needed. In this study, the one-domain coupling method has been utilized to study the effects of the porous medium on the evaporation of multi-phase liquids. One-domain coupling method needs a single governing equation applicable to porous and free-flow regions.

In this study, the CFD method has been utilized to analyse the rate of evaporation from a porous media as a function of temperature, heat transfer, inlet free-flow velocity, the saturation of multi-species liquids, and the porous medium structure. The obtained data for evaporation in the case of the porous media is validated against the model with a direct liquid interface with no porous media. Hence, a quantitative estimation of the evaporation of different components has been put forward.

Acknowledgements

Writing this thesis was a hard job, and it would have been impossible without the support of various people.

- First, I would like to express my sincere appreciation towards my co-supervisors, Thorsten Jonach and Dr Bahram Haddadi, for their continuous support to my work through guidance and keeping me on track.
- I am also grateful to my supervisor Michael Harasek for accepting me into his research team and supporting me throughout my research work.
- I want to thank all the professors under whom I had the pleasure to study at TU Wien and University of L'Aquila.
- I am also grateful to my "MathMods" friends, who helped me learn and tackle this intense master's program.
- Last but not least, I would like to thank my parents. Without their belief and emotional support, this would have been impossible to conquer.

Contents

Declaration of Authorship	ii
Abstract	iii
Acknowledgements	iv
List of Figures	vii
List of Tables	ix
1 Introduction	1
1.1 Background	1
1.2 Aim and Objectives	2
2 Literature Review	3
2.1 Porous Media: A Glance	3
2.1.1 Terms and Definitions in Porous Media	3
2.2 Evaporation	6
2.2.1 Kinetic Theory of Gases	6
2.2.2 Evaporative Equilibrium	7
2.2.3 Saturated Vapor Pressure	7
2.2.4 Raoult's Law	8
2.3 Summary of the Chapter	8
3 Transport through Porous Media	9
3.1 Assumptions in Modelling of Flow	10
3.2 Forces Influencing the Fluid Flow	10
3.2.1 Capillary Force	11
3.2.2 Viscous Force	11
3.3 Conservation Equations	12
3.3.1 Mass Conservation Equation	12
3.3.2 Momentum Conservation Equation	13
Darcy's Law	13
Forchheimer's Equation	14
Navier-Stokes Equation for Porous medium flow	15
3.3.3 Energy Conservation Equations	16
3.4 Volume Averaging	16
3.4.1 Averaging of Mass Conservation Equation	18
3.4.2 Averaging of Momentum Conservation Equation	18
3.4.3 Averaging of Energy Conservation Equation	18
3.5 Summary of the Chapter	19

4 Evaporation through Porous Media	20
4.1 Drying Stages	20
4.1.1 Stage-I	21
4.1.2 Stage-IIa	21
4.1.3 Stage-IIb	22
4.2 Review of Prior Models	22
4.2.1 Single-Domain Coupling Model	23
4.2.2 Two-Domain Coupling Model	24
4.2.3 Evaporation Models on REV	25
4.3 Mathematical Modelling of Coupled Evaporation	25
4.3.1 Bouddour Model [3]	25
4.3.2 Zhang Model [41]	26
4.4 Summary of the Chapter	29
5 Numerical Modelling	30
5.1 OpenFOAM	30
5.2 porousEvapFoam: An OpenFOAM Solver	30
5.2.1 Momentum Conservation Model	30
Calculation of Coefficients	33
5.2.2 PIMPLE Algorithm	33
5.2.3 Courant Number	34
5.3 Discretization of Momentum Equation	35
5.3.1 Temporal Term	35
5.3.2 Convection Term	35
5.3.3 Pressure Term	36
5.3.4 Diffusion Term	36
5.3.5 Sink Term	36
5.4 Numerical Schemes	36
5.4.1 Time Schemes	37
5.4.2 Gradient Schemes	37
5.4.3 Divergence Scheme	37
5.4.4 Laplacian Schemes	38
5.5 Simulation Case Setup	38
5.5.1 Geometry Setup	38
5.5.2 Mesh	39
5.5.3 Initial, Boundary Conditions	39
5.6 Summary of the Chapter	41
6 Results and Discussions	42
6.1 Porous Media Effect on Evaporation	42
6.2 Porous Media Flow Results	43
6.3 Temperature Effect on Evaporation	45
6.4 Evaporation Effect on Free Flow	46
6.5 Multiprocessor Simulation Results	48
6.6 Computation Time Comparison	48
7 Conclusions and Future Work	50
Bibliography	51

List of Figures

1.1 Evaporation from Earth's surface can be illustrated as an example of evaporation from the porous medium with complex interactions with the environment [18]	1
2.1 Different scales of Porous Media based on different applications [40]	4
2.2 REV for Porosity	4
3.1 Illustration of flow through rigid porous media	9
3.2 Capillary effect of Multiphase Fluids [21]	11
3.3 Advantages and limitations of the different porous flow models	15
3.4 Illustration of volume averaging, with solid and fluid volumes V_s and V_f , respectively, in an arbitrary porous media [7]	17
4.1 Illustration of evaporation from Porous Media [26]	20
4.2 Qualitative illustration of different stages of drying rate from a porous media [7]	21
4.3 Description of Coupling at Interface [29]	23
4.4 Single domain approach using Brinkman equation with a transition zone	23
4.5 Two-Domain coupling approach with sharp interface and strong coupling condition	24
5.1 Flowchart of Evaporation in porousEvapFoam solver	31
5.2 Structure of porousEvapFoam Solver	31
5.3 Overall flowchart of porousEvapFoam solver for multi-region	32
5.4 Flowchart for PIMPLE Algorithm [31]	34
5.5 Front View of the sample Geometry	38
5.6 Mesh of the geometry generated using <i>blockMesh</i>	39
5.7 Openfoam Coupling between Solid and Fluid Regions	40
6.1 Comparison of the beginning of evaporation of two cases	42
6.2 Comparison of evaporation of liquids at the outlet	43
6.3 Flow of multi-species liquids within porous media towards drying front at different time	44
6.4 Proportion of liquid species in the porous media at different intervals due to drying from porous media	44
6.5 Evolution of the temperature in the free-flow regime at a point near the heater	45
6.6 Variations of the proportion of each component with temperature	45
6.7 Proportion of each component in the gaseous region at $t = 3s$	46
6.8 Proportion of each component in the gaseous region at $t = 8s$ and $t = 30s$	46
6.9 Proportion of each component in the gaseous region at $t = 60s$ and $t = 100s$	47

6.10 Proportions of each components at different time intervals	47
6.11 Runtime of simulation on various no. of processors	48
6.12 Curve for the run time vs. number of cells	49

List of Tables

5.1	OpenFoam Schemes for time discretization	37
5.2	OpenFoam Schemes for gradient	37
5.3	OpenFoam Interpolation schemes for divergence	37
5.4	Number of cells in each region	39
5.5	Initial and boundary conditions for fluidDomain	40
5.6	properties of the heater used for Simulation (arbitrary material)	40
5.7	Properties of Arbitrary liquids specieA and specieB	41
6.1	The run time of simulation with several numbers of cores	48
6.2	The run time of simulation with various number of Cells on 2 processors	49

List of Abbreviations

CFD	Computational Fluid Dynamics
REV	Representative Elementary Volume
Re	Reynold's Number
Da	Darcy's Number
DNS	Direct Numerical Simulation
LBM	Lattice-Boltzmann Method
VoF	Volume of Fluid
NSE	Navier-Stokes Equation
OpenFOAM	Open Field Operation And Manipulation
PDE	Partial Differential Equation
FVM	Finite Element Volume
OF	OpenFOAM
OF9	OpenFOAM Version 9
RAS	Reynolds Averaged Simulation
LES	Large Eddy Simulation
SIMPLE	Semi-Implicit Method for Pressure-Linked Equations
PISO	Pressure-Implicit with Splitting of Operators
CFL	Courant-Friedrichs-Lowy
QUICK	Quadratic Upstream Interpolation for Convective Kinematics
CV	Control Volume

List of Symbols

Φ	Porosity
V_b	Bulk Volume of Porous Media (m^3)
V_p	Void Volume of Porous Media (m^3)
s	Specific Internal Area (m^{-1})
τ	Tortuosity
k	Boltzmann Constant (J/K)
P	Pressure (N/m^2)
T	Temperature (K)
R	Universal Gas Constant ($NmK^{-1}mol^{-1}$)
x	Mole Fraction
σ	Surface Tension (N/m)
ρ	Density (kg/m^{-3})
β	Extensive Properties
b	Intensive Properties
S	Saturation
Q	Volume Flow Rate (m^3/s)
K	Permeability Coefficient (m^2)
μ	Dynamic Viscosity of Fluid ($kg/(m * s)$)
ν	Kinematic Viscosity of Fluid (m^2/s)
μ_{eff}	Effective Viscosity of Fluid ($kg/(m * s)$)

ω	Mass Fraction
h	Heat Transfer Coefficient ($W / (m^2 * K)$)
E_a	Activation Energy (J)
S_m	Sink
D	Darcy's Coefficient
F	Forchheimer's Coefficient
C_F	Dimensionless Forchheimer Coefficient
Co	Courant Number
B	Carman-Konezy Constant

Chapter 1

Introduction

1.1 Background

Evaporation from porous media is one of the critical processes relevant to many engineering, environmental and hydrological processes, such as drying of building materials, baking, and water purification. It is also one of the vital processes, maintaining the hydrological cycle and managing the mass exchange between the atmosphere and the earth's surface. In the last century, research in this field has grown enormously due to its vast applications in most engineering fields. Thus, it is of utmost importance to understand the controlled evaporation from porous media under provided boundary conditions.

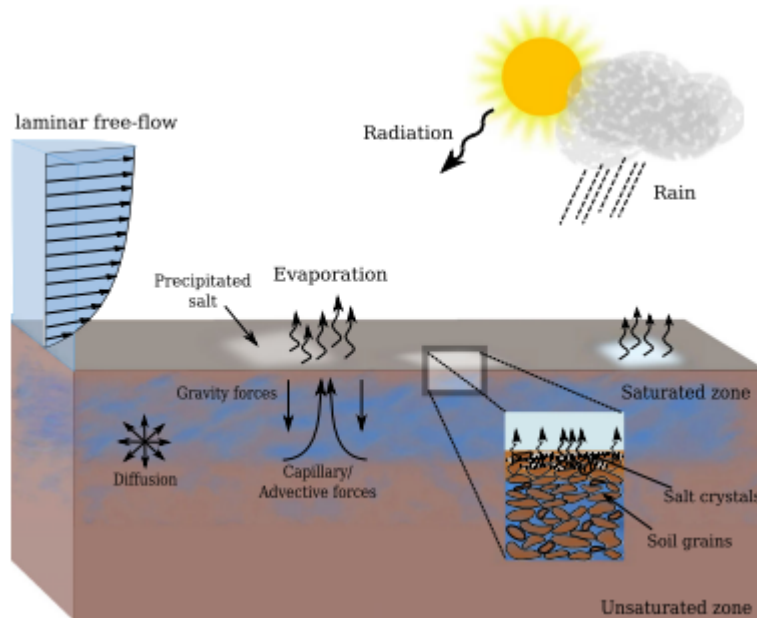


FIGURE 1.1: Evaporation from Earth's surface can be illustrated as an example of evaporation from the porous medium with complex interactions with the environment [18]

Evaporation within the porous medium involves multiple complex processes such as simultaneous heat and mass transfer, phase changes at the surface and within the medium, and liquid and gaseous displacement at pore scales which are difficult to describe. The process becomes more complex while dealing with multi-species liquids. Due to the impact of these processes, the flow dynamics within the porous medium and the free stream exhibit strong dependencies. These dependencies are often controlled by the mechanisms at the interface, separating porous

medium and free flow. To better describe possible applications in which evaporation from porous media plays a decisive role, this simultaneously occurring phenomenon must be summarized.

The vapour pressure difference at the interface is the major driving cause of evaporation. Another cause is the speed of flow over the interface in free flow. The higher free flow rate causes the liquid molecules to carry away from the porous media interface. The energy is required for evaporation to occur. It can be transferred to the system through radiation or temperature differences.

1.2 Aim and Objectives

Motivated by the importance of understanding and controlling the evaporation from the porous media with its vast engineering applications, this thesis focuses on the evaporation of liquids within a saturated porous media to the free-flow region through the common interface. The main objective of this research work is to implement the models of porous media flow and evaporation within the framework of OpenFOAM. The following sub-targets are, therefore, put forward:

- Understanding different models of porous media evaporation by a thorough literature review.
- Model implementation and simulation within the OpenFoam framework.
- Quantitative comparison of the effects of porous media on the rate of evaporation.

Chapter 2

Literature Review

2.1 Porous Media: A Glance

Porous materials are experienced all over in technological innovations and nature. Except for every metal, dense rocks, and a few artificial plastics, most solids and semi-solids are virtually *porous* to a certain degree.

A porous medium can be introduced as the (almost) fixed solid matrix with or without multiply connected void spaces. The support skeleton part of the solid material is commonly known as the matrix, which can undergo small deformations. A porous medium should possess at least one of the following properties:

1. It should contain spaces (termed as pores or voids) embedded within the semi-solid or solid matrix.
2. Different fluids should be able to pass through the material volume.

In case holes and pores within a solid domain will reduce the material's strength, then it is a design fault. In that case, the material cannot be called *porous*. Tiny spaces between the molecules in a solid are called *molecular interstices*, and huge spaced ones are called *caverns*. The void sizes between molecular interstices and caverns are called pore space.

The pore spaces in the porous media can be either *interconnected* or *non-interconnected* based on the materials. The interconnected void space means the pore spaces are connected through a continuous void network. If the pore space is non-connected, it is termed a non-interconnected void.

2.1.1 Terms and Definitions in Porous Media

First, fundamental terms must be defined to deal with fundamental physical processes and material properties in the context of modelling and analysis of complex processes of coupled transport and evaporation from porous media due to heat transfer and free flow of air.

(1) Scales

Different scales are needed to describe the flow phenomena in a porous media. The typical scales used in the porous media are the pore scale, REV scale and field scale. Different scales are shown in Figure 2.1.

The so-call *Representative Elementary Volume* (REV) is the most crucial scale for the porous media. On the REV scale, average pore space is considered to be consistent.

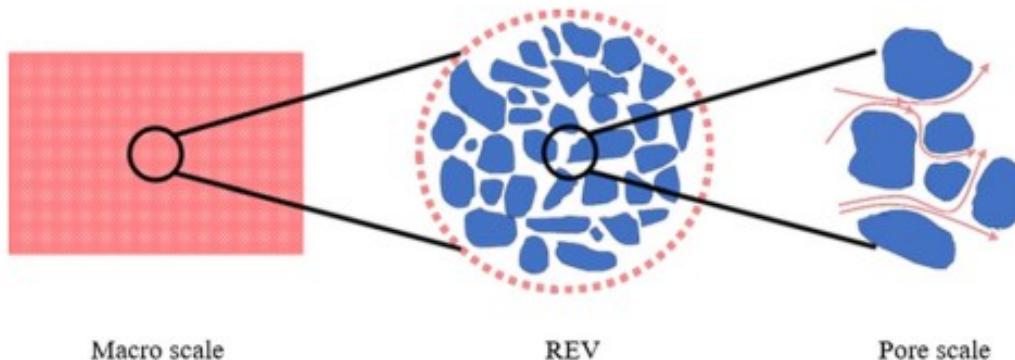


FIGURE 2.1: Different scales of Porous Media based on different applications [40]

Modelling of the transport in porous media is based on the REV scale. However, the size of the REV cannot be chosen randomly but has to be a range where the average quantity on the volume averaging would lead to the same value of a fraction of pore space, as shown in Figure 2.2.

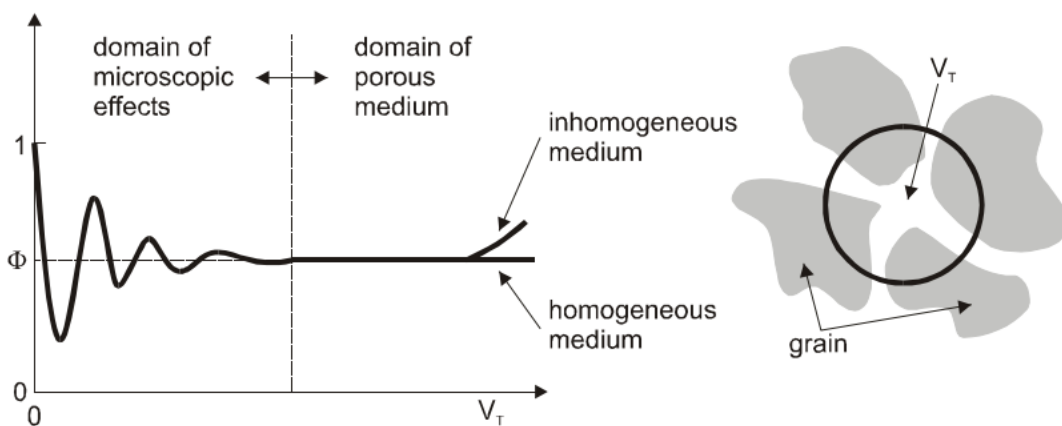


FIGURE 2.2: Representative Elementary Volume for Porosity [14]

(2) Porosity

The porosity of a porous media can be characterized quantitatively as the proportion of the void space to the whole volume of the permeable space in consideration.

Due to the connected pore network, which allows fluid flow in porous media, interconnected voids are essential in fluid flow in the porous medium. In this regard, *effective porosity* is considered instead of porosity. Quantitatively, effective porosity can be given by:

$$\phi = \frac{V_p}{V_b} \quad (2.1)$$

where V_p represents the interconnected void spaces and V_b is the bulk volume of the porous material.

Effective porosity can range from 0.6 for natural materials to 0.99 for some advanced manufactured materials [30]. This porosity allows the flow of fluids through the media. So, in porous media, different material constituents are arranged in an unordered fashion.

Porosity is a statistical quantity, depending on the magnitude of the volume of the bulk. On REV scale, porosity is function of space.

(3) Specific Internal Area

Another property of the porous material is the *specific internal area*. It is defined as the fraction of the total internal area of the porous material to the bulk volume of the porous materials. Due to this reason, it is expressed as the reciprocal of the specific length.

$$s = \frac{A_{in}}{V_b} \quad (2.2)$$

where A_{in} is the internal surface area and V_b is the bulk volume of the porous material.

(4) Tortuosity

Tortuosity can be defined as the ratio of the actual flow path length through interconnected pores to the closest distance between the ends of the flow path [2]. It is an intrinsic and kinematic property of the porous material.

$$\tau = \frac{L_t}{L} \quad (2.3)$$

where L_t is the tortuous fluid pathways, and L is the length of the bulk porous material.

(5) Phase

Since there is consideration of multi-species fluid flow through a porous media, it is necessary to introduce the phases of fluids and solids separately. A phase can be introduced as a distinct, continuous and homogeneous state of a system with no visible boundary (interface). On a continuum scale, the physical state of a phase is characterized by thermodynamic factors such as pressure, temperature or density. Multiple phases are usually separated from each other through interfaces.

(6) Interface

In the multi-species system of flow and evaporation along with porous regions, interfaces are involved in different scales.

- Liquid-gas interface
- Multi-component liquids interface
- Porous medium-liquid interface
- Porous media-free flow interface

Interfaces are usually thin transition zone between different phases.

2.2 Evaporation

Evaporation can be introduced as the vaporization of a liquid that occurs at the surface of the liquid as it changes from the liquid phase to the gaseous phase. Evaporation is directly proportional to the liquid-gas interface surface. In most cases, the interface is small compared to the volume of liquid. Hence, only a fraction of molecules in liquid can have enough energy to escape from it. The evaporation is continued till it reaches equilibrium. Equilibrium is achieved when the rate of evaporation equals the rate of condensation. A liquid evaporates in a closed environment until the surrounding air is saturated. The molecules in the liquid phase collide; they transfer energy to each other due to collision and temperature differences. When the molecule near the interface absorbs enough energy to overcome the vapour pressure and surface tension, they escape and enter the surrounding air. When evaporation occurs, the energy has been taken out from the liquid phase due to the vaporization of liquid molecules. It will reduce the temperature of the liquid, resulting in evaporative cooling.

A deep study of the evaporation of liquid starts at the liquid-gas interface. However, the transport of liquid molecules to the gaseous phase begins with the kinetic theory of gases.

2.2.1 Kinetic Theory of Gases

It is a simple and significant classical model to describe the thermodynamic behaviour of gases. The model introduces a gas as the collection of huge numbers of identical sub-microscopic particles, all in constant, rapid and random motion.

The kinetic theory of gases consists of various postulates and assumptions that:

- Any gas consists of like or unlike micro-particles, called molecules
- These molecules can move in all directions randomly
- Molecules cause the pressure in the gaseous phase due to the constant impact of molecules
- The pressure is caused by the constant impact of molecules on the boundary of the container
- The collisions between molecules within the gaseous region are perfectly elastic (no energy transfer)
- All molecules follow the general laws of motion

The average molecular velocity can be calculated by the Maxwell-Boltzmann probability distribution function [22] given by

$$P(c)dc = 4\pi \sqrt{\left(\frac{m}{2\pi kT}\right)^3} \exp\left(-\frac{mc^2}{2kT}\right) c^2 dc \quad (2.4)$$

where $P(c)dc$ is the probability that the molecules have speed c in speed range dc , m is the mass of the molecule, k is the Boltzmann constant, and T is the absolute temperature.

On the molecular level, there is no strict boundary between the liquid and vapour states. Instead, there exists a Knudsen layer [24], where the phase is undetermined. Since this layer is only a few molecules thick, a clear phase transition cannot be visualized on the macroscopic scale.

2.2.2 Evaporative Equilibrium

When evaporation occurs in a confined container, the fleeing molecules collect as vapours above the liquid. Some of the molecules revert back to the liquid more often as the density and pressure of the vapour increase. The process of exchange of the molecules between the liquid and gaseous phases depends on the temperature. When the rate of molecules leaving the liquid phase to the gaseous phase equals the rate of molecules reverting back to the liquid phase from the gaseous phase, the system is in *equilibrium*. In that case, the pressure of the system attains its peak at that temperature.

For a pure substance, the equilibrium state is directly proportional to the vapour substance and can be given by the Clausius-Clapeyron equation [25] as

$$\ln\left(\frac{P_2}{P_1}\right) = -\frac{\Delta H_{vap}}{R} \left(\frac{1}{T_2} - \frac{1}{T_1} \right) \quad (2.5)$$

where P_1 and P_2 are the vapour pressure at T_1 and T_2 , respectively, ΔH_{vap} is the enthalpy of vaporization, and R is universal gas constant.

The maximum possible number of molecules leaving per unit area of a liquid per second when the liquid is in equilibrium can be calculated as [23]

$$\Phi_s = \frac{P_s}{\sqrt{(2\pi mkT_s)}} \quad (2.6)$$

where Φ_s is the maximum possible number of molecules leaving the liquid surface, P_s is saturation vapour pressure over the liquid surface, T_s is the saturation temperature, and k is the Boltzmann constant.

2.2.3 Saturated Vapor Pressure

One major reason for evaporation is the difference in the equilibrium vapour pressure in different phases (gaseous and liquid). When the equilibrium vapour pressure (aka saturated vapour pressure) of the two phases equals the partial vapour pressure exerted by the gaseous phase to the liquid phase. This saturated vapour pressure depends strongly upon the temperature. This relationship can be given by Kelvin equation [8] as

$$p_g^l(T) = p_{sat}^l \exp\left(-\frac{p_c}{\rho RT}\right) \quad (2.7)$$

where ρ is the density of the fluid, R is the universal gas constant, and T is the temperature.

When fluid and vapour stages are in balance, the mole fractions of each component within the vapour phase can be calculated as follows:

$$x_g^l = \frac{p_g^l}{p_g} \quad (2.8)$$

where x_g^l is the mole fraction of the gaseous phase, p_{sat} is the saturated partial pressure of the component and p_g is the partial pressure in the gaseous phase.

2.2.4 Raoult's Law

For multi-species fluids, the partial pressure p_g^i of the i^{th} component in the gaseous phase is given as the mole fraction of component i within the liquid phase x_l^i by Raoult's Law.

Raoult's law can be expressed as

$$p_g^i = x_l^i p_{sat} \quad (2.9)$$

where p_{sat}^i is the saturated vapour pressure.

The total pressure of the system can be given by:

$$P = \sum_{i=1}^n p_g^i \quad (2.10)$$

where P is the total pressure of the system and p_g^i is the individual components pressure.

2.3 Summary of the Chapter

We have already looked into the porous media and evaporation. Due to engineering applications, it is vital to understand the drying of porous media. In porous media, the distribution of porosity, permeability and structure of porous material play significant roles in determining the dynamics of the evaporation.

Flow through porous media is crucial for evaporative drying. A detailed dynamics of flow through porous media is presented in chapter 3. In general, evaporation from porous media is grouped into two different stages: the constant evaporation rate period, and the falling rate period. We will see the detailed about the evaporation dynamics in chapter 4.

Chapter 3

Transport through Porous Media

The fluid flow inside and over the porous media is intrigued in numerous natural and engineering regions. This is because porous media is quite commonly available in nature and have brought many applications in modern engineering. Examples are the flow of hydrocarbons on the earth's surface, groundwater flow, and transport of contaminants in the ground. Some engineering examples that play vital roles are geothermal energy storage, solidification of molten alloys, heat-exchanger technologies and lubrication.

Porous media flow is usually laminar. But, it usually follows the tortuous path, based on the pore network of interconnected voids. The study of flow and distributions of the physical quantities with the porous domain constitutes the *transport in the porous medium*.

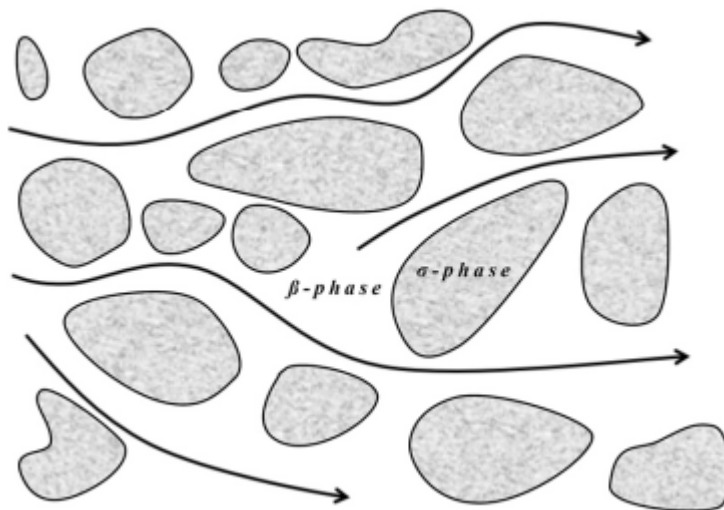


FIGURE 3.1: Illustration of flow through rigid porous media

Different flow paths can be obtained in the permeable medium, managed by flow regimes (such as laminar or turbulent, steady or unsteady), interfaces in multi-phase flow, phase change phenomena, and transported variables non-equilibrium phenomena. Furthermore, flow patterns and transport depend on pore and solid micro-structures.

In previous works, different methods have been employed to study transport phenomena in the non-uniform porous medium as follows:

1. **Deterministic Model:** Governing equations formulation for non-homogeneous, anisotropic region, treating permeability and porosity as second-order tensors (depending on spatial location).
2. **Stochastic Model:** Statistics/stochastic methods accounting for fluctuations in physical quantities with respect to spatial locations, treating permeability and porosity as arbitrary variables with well-described mean values.

A deterministic model can be traditionally solved using numerical methods, while a stochastic model needs to solve multiple times to generate a resulting flow and scalar field realization. However, one of the most significant hurdles encountered in both approaches depends on the sensitivity of the numerical solutions relative to the pore-scale variations in the macroscopic behaviours. To be precise, a finer meshing of the geometry will permit a more reliable pore structure, providing completely new solutions. If you increase the scale for laboratory realizations, then variations are entirely masked. If transport occurs at larger scales in porous media, then this difficulty of realization is compounded. Past approaches have been proposed in a way that only some of the goals of mathematical models are realized, and remaining are compromised.

3.1 Assumptions in Modelling of Flow

Certain assumptions are enforced to develop simple mathematical models for the transport from the porous medium. They are:

- The solid material matrix is fixed and cannot be deformed or moved.
- Void space is also fixed and has a structure independent of time.
- Only fluid flow decides the flow dynamics.
- The characteristics dimension of the void space is minimal compared to the total porous medium domain.

3.2 Forces Influencing the Fluid Flow

Transport within a porous media is a complex physical problem where many factors are affecting the fluid flow within the porous media matrix. Major forces affecting the fluid flow phenomena must be considered in the mathematical modelling. Major forces which are affecting the characteristics of the fluid flow through the porous media are:

- Capillary force
- Viscous force
- Gravity force

3.2.1 Capillary Force

Capillary action in the porous media is one of the most important forces leading to significant variations if not considered in modelling the fluid flow. Considering the case of a candle, the melted wax moves up through the porous thread by the action of the capillary rise only. Capillary forces can be influenced by the gravity effect and density of the fluid. In general, considering the porous medium to be non-wetting, the capillary pressure can be calculated as follows:

$$P_c = \frac{2\sigma \cos\theta}{r_c} \quad (3.1)$$

where, σ is the surface tension on solid-fluid interface, θ is the contact angle between the fluids and porous media, and r_c is the radius of the average pore space.

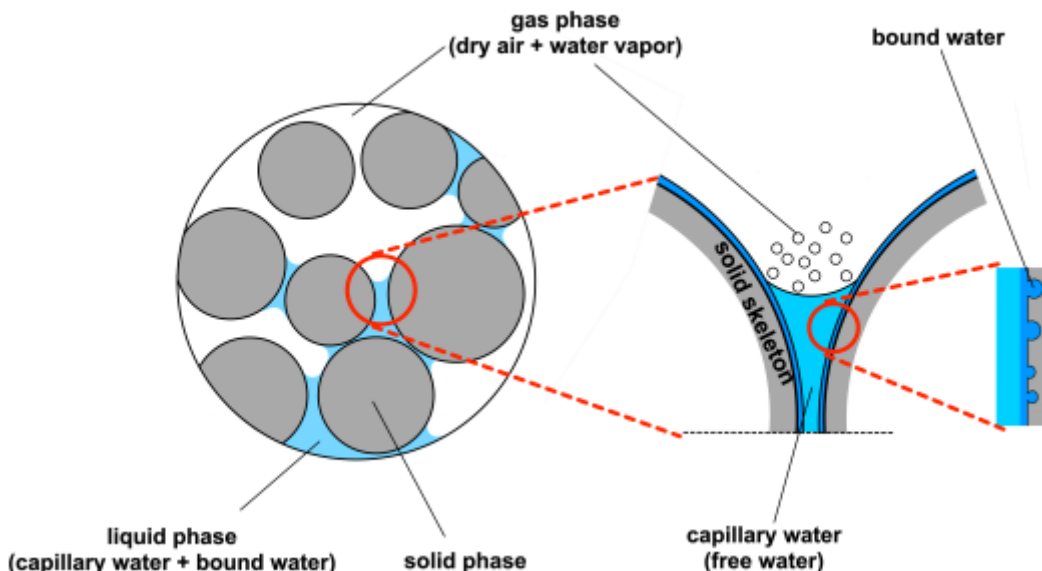


FIGURE 3.2: Capillary effect of Multiphase Fluids [21]

In the case of immiscible multi-species fluids, the pressures at both sides of the interface are not equal, giving rise to the capillary pressure P_c , which can be calculated by the Laplace equation as

$$P_c = \sigma_{12} \left(\frac{1}{r_1} + \frac{1}{r_2} \right) \quad (3.2)$$

where σ_{12} is the net surface tension between different phases and r_1 and r_2 are principle curvatures radii.

3.2.2 Viscous Force

Since the fluid in the motion is not considered to be ideal fluid, a viscous force exists between different layers of the fluid. Viscous force comes into existence whenever there is relative motion between layers. Viscous force is calculated by Newton's law of viscosity, given as follows:

$$\tau = \mu \frac{du}{dy} \quad (3.3)$$

where τ is shear stress, μ is coefficient of viscosity, and $\frac{du}{dy}$ is shear strain rate.

Viscous forces are generated due to different cohesive and adhesive forces between different phases of the multi-species non-homogeneous flow in the porous media. In most of the multi-phase flows in porous media, viscous forces dominate other fluid flow mechanisms.

3.3 Conservation Equations

Reynolds transport equation [32] states that the time rate of change in an extensive quantity β equals the sum of the rate of change of an intensive quantity $b = d\beta/dm$ within the control volume (CV) Ω and net rate of change of the same intensive quantity across the boundary Γ of control volume (CV), given as

$$\frac{d\beta}{dt} = \int_{\Omega} \frac{\partial(\rho b)}{\partial t} d\Omega + \int_{\Gamma} (\rho b)(v \cdot n) d\Gamma \quad (3.4)$$

where β is an extensive quantity, m is mass, n is the unit vector perpendicular to the surface Γ .

3.3.1 Mass Conservation Equation

Reynolds transport equation 3.4 can be used to derive the conservation of mass equation with the consideration of extensive property $\beta = m$. In this case, intensive property $b = dm/dm = 1$. Hence, equation 3.4 can be re-written as:

$$\frac{dm}{dt} = \int_{\Omega} \frac{\partial \rho}{\partial t} d\Omega + \int_{\Gamma} \rho(v \cdot n) d\Gamma \quad (3.5)$$

Using Gauss divergence theorem to change surface integral in RHS to volume integral, given as:

$$\int_{\Gamma} \rho(v \cdot n) d\Gamma = \int_{\Omega} \nabla \cdot (\rho v) d\Omega \quad (3.6)$$

which changes equation 3.5 into the form

$$\frac{dm}{dt} = \int_{\Omega} \frac{\partial \rho}{\partial t} d\Omega + \int_{\Omega} \nabla \cdot (\rho v) d\Omega \quad (3.7)$$

For infinitesimally small control volume, mass conservation equation can be written as:

$$\boxed{\frac{\partial \rho}{\partial t} + \nabla \cdot (\rho v) = 0} \quad (3.8)$$

The general conservation of mass equation with porosity ϕ with the fluid phase α in the porous media with the saturation S_α can be written as:

$$\boxed{\frac{\partial(\phi S_\alpha \rho_\alpha)}{\partial t} + \nabla \cdot (\rho_\alpha v_\alpha) - \rho_\alpha q_\alpha = 0} \quad (3.9)$$

where q_α is source/sink of the phase α into the system.

3.3.2 Momentum Conservation Equation

Darcy's Law

By the observations made by Darcy on the city supply water in Dijon, he suggested Darcy's law after experimenting on steady, linear flow in porous media [9], given a simple relation as:

$$Q = K \cdot \frac{S}{L} \cdot h \quad (3.10)$$

where Q is flow rate, K stands for permeability coefficient, S is the cross-section of the packing, L is the length, and h is pressure head.

With developments in later years, Darcy's law can be given in the modern form:

$$-\nabla p = \frac{\mu v}{K} \quad (3.11)$$

where p is pressure, v is velocity, μ is dynamic viscosity of the fluid, and K is the porous medium permeability. Here v is related to the porosity of the medium ϕ as $v = \phi V$ with V equals the average velocity through the porous media domain.

In the modern form for numerical models of multi-species system, Darcy's law 3.11 can be rewritten as:

$$v = -K \frac{1}{\mu} (\nabla p + \rho g) \quad (3.12)$$

where K is the porous medium permeability, μ is fluid's dynamic viscosity, p is the pressure, and g is gravity.

Considering equation 3.12, Darcy's law can be written for different phases as [34]:

$$\begin{aligned} v_\alpha &= -\frac{1}{\mu_\alpha} K_\alpha (\nabla p_\alpha - \rho_\alpha g) \\ &= -\frac{K_{\beta\alpha}}{\mu_\alpha} K_\alpha (\nabla p_\alpha - \rho_\alpha g) \\ &= -\lambda_\alpha K (\nabla p_\alpha - \rho_\alpha g) \end{aligned} \quad (3.13)$$

where v_α is called phase velocity, α is different phases in the multiphase system, K denotes permeability, $K_{\beta\alpha}$ denotes relative permeability, and λ_α is called mobility.

Darcy's law is applicable in the case of steady and linear flow for the low Reynold's numbers. In *unsteady* and *linear* flows, inertial acceleration of the fluid causes different directions for pressure gradient and mean velocity. It can be represented by the time derivative of mean velocity and can be given as *unsteady Darcy equation* [5]:

$$-\nabla p = \frac{\mu v}{K} + \gamma \frac{\partial v}{\partial t} \quad (3.14)$$

where coefficient γ represents the inertial term due to acceleration due to flow.

Further correction in *Darcy's equation* was suggested by Brinkman [4]. He observed that the predicted velocity components by Darcy's law are independent of the axial directions, meaning they are *fully developed*. So, if the pressure gradient

changes with respect to time, the velocity component should not change drastically because only pore diameter decides transient duration and flow development. Also, it abuses the no-slip condition between the fluid and solid boundaries, commonly observed in continuum fluid flow. Also, porous media leads to extremely skinny wall boundary layers at the pore-scale. So Brinkman [4] gave a correction in Darcy's equation:

$$-\nabla p = \frac{\mu v}{K} - \frac{\mu}{\phi} \Delta v \quad (3.15)$$

where μ represents the effective viscosity, K is the permeability, and ϕ is the porosity of the porous media.

Forchheimer's Equation

Darcy's law is based on the assumption that the rate of fluid flow in a porous media is proportional to pressure gradient. But the limitation of this law is that it is valid only for small velocities (small Reynolds number). At higher velocities (high Reynolds number), turbulence may develop, leading to the failure of Darcy's law as additional pressure drop may appear compared to what is predicted by this law. Forchheimer [11] devised a empirical relation based on the several experimental and theoretical investigations. He found the quadratic relation between drag in the porous media to velocity of flow. Forchheimer equation can be given as:

$$-\nabla p = \frac{\mu v}{K} + F \rho v^2 \quad (3.16)$$

where F is the Forchheimer coefficient, and ρ is the fluid density. In this equation, 2nd term in RHS represents the kinetic energy due to the inertial effect. For a particular case when particles are spherical, then Forchheimer coefficient F can be given by the relation [6]:

$$F = B \frac{(1 - \phi)}{D_p \phi^3} \quad (3.17)$$

where ϕ is porosity and B is constant and is equal to 1.75 (or 1.80 for packed bed) based on Carman-Konezy relations [6].

Altogether Brinkman and Forchheimer-corrected Darcy's law can be represented as:

$$-\nabla p = \frac{\mu v}{\kappa} + F \rho v^2 - \frac{\mu}{\phi} \Delta v \quad (3.18)$$

The above equation is a momentum equation in which the total effects of fluid pressure, viscous forces at the fluid-solid boundary, viscosity within multi-phase fluids, and form drag are attained at the REV scale.

Hsu et al. [16] worked on the medium range of *Reynolds number* and suggested to add another compensating term along with the Forchheimer term to take into the consideration for viscous boundary layer effects. It can be given as follows:

$$-\nabla p = \frac{\mu v}{\kappa} + A \sqrt{\rho \mu v} + F \rho v^2 \quad (3.19)$$

where A accounts for quantity, which is a function of porosity.

Unsteady and *non-linear* flows can be represented by *unsteady Forchheimer equation* used by many researchers [5, 13] and can be given as:

$$-\nabla p = \frac{\mu v}{\kappa} + \beta \rho v^2 + \gamma \frac{\partial v}{\partial t} \quad (3.20)$$

Here all mentioned terms have usual meaning as mentioned before.

Porous Flow Models	Advantages	Limitations
Darcy's Law	Steady and linear flows	Applicable to $Re < 10$
Unsteady Darcy's Law	Unsteady and linear flows, consideration of inertial acceleration of fluid	Applicable to $Re < 10$
Darcy-Brinkmann Equation	Steady and linear flows, consideration of no-slip on solid boundary	Applicable to $Re < 10$
Forchheimer Equation	Applicable to wide range of Reynolds number	Determination of coefficient β is difficult
Darcy-Forchheimer-Brinkmann Equation	Applicable to wide range of Reynolds number and considers the no-slip condition at pore boundary	No consideration of Boundary layers at pore boundary
Hsu Equation	Applicable to high Reynold's number and Boundary layer consideration on pore boundary	

FIGURE 3.3: Advantages and limitations of the different porous flow models

Navier-Stokes Equation for Porous medium flow

The Navier-Stokes equation (NSE) for incompressible flows can be used to derive the equation of fluid flow through the porous medium. The equation can be given as [10]:

$$\frac{\rho}{\phi} \left[\frac{\partial v}{\partial t} + \frac{1}{\phi} (\nu \cdot \nabla \nu) \right] = - \frac{\partial p}{\partial x} + \tilde{\mu} \frac{\partial^2 \nu}{\partial x^2} - \frac{\mu \nu}{\kappa} - \frac{C_F \rho}{\kappa^{1/2}} \nu^2 \quad (3.21)$$

The above equation 3.21 can be applied to the incompressible fluid with density ρ , effective viscosity $\tilde{\mu}$, and Forchheimer coefficient in dimensionless form C_F . If gravity effects are not negligible, then the pressure term can be replaced by effective pressure. This *effective pressure* is the net pressure, considering all pressure terms such as capillary pressure, fluid pressure and pressure head due to gravity. This approach can be applied to all types of body forces.

Extending the equation for non-dimensionalization, considering L to be macroscopic length scale, and U velocity scale for setup. Reynold's number can be given as

$$Re = \frac{\rho U L}{\mu} \quad (3.22)$$

And non-Darcy model equation can be given in dimensionless form as

$$\boxed{\frac{1}{\phi} \left[\frac{\partial v}{\partial t} + \frac{1}{\phi} v \cdot \nabla v \right] = -\frac{\partial p}{\partial x} - \frac{1}{Re \times Da} v - \frac{f}{\sqrt{Da}} v^2 + \frac{1}{\phi Re} \frac{\partial^2 v}{\partial x^2}} \quad (3.23)$$

where Da is Darcy's number, which is defined as:

$$Da = \frac{K}{L^2} \quad (3.24)$$

3.3.3 Energy Conservation Equations

Various formulations are possible for the conservation of the energy. Here, considering the formulation based on the phase enthalpy and internal energy as:

$$\frac{\partial(\rho_\alpha v_\alpha)}{\partial t} + \nabla \cdot F_h - q_h = 0 \quad (3.25)$$

with the internal energy of the phase α and heat flux is given as

$$F_h = \underbrace{\rho_\alpha h_\alpha v_\alpha}_{\text{convection}} - \underbrace{\lambda_\alpha \nabla T}_{\text{conduction}} - \underbrace{\sum_i D_\alpha^i \rho_\alpha \nabla x_\alpha^i h_\alpha^i}_{\text{diffusion heat transfer}} \quad (3.26)$$

where λ_α is the thermal conductivity of the phase, h_α is phase enthalpy, and q_h is source/sink.

The governing equations at the pore scale for a porous medium with solid and fluid phases can be given as:

$$\rho_f c_{pf} \left(\frac{\partial T_f}{\partial t} + v \cdot \nabla T_f \right) = k_f \Delta T_f \quad (3.27)$$

and

$$\rho_s c_s \frac{\partial T_s}{\partial t} = k_s \Delta T_s \quad (3.28)$$

where f and s are subscripts for solid and fluid phases, respectively. The specific heat capacities are denoted as $c_{p,f}$ and c_s , respectively. k represents the thermal conductivities of the respective phase.

We have discussed till now about the micro-scaled conservation equations for the transport with the porous media. We will discuss now the conservation equations for transport on the REV scale. But, before heading to the derivation of conservation equations on REV, we need to define the volume averaging method, the mathematical tool used to derive the conservation equations on REV.

3.4 Volume Averaging

The method of volume averaging is a mathematical formulation through which the governing conservation equations in a porous medium are volume averaged on a REV to obtain an averaged set of governing equations of transport in the porous medium. It was introduced by Whitaker [39] and further refined by Gray [12].

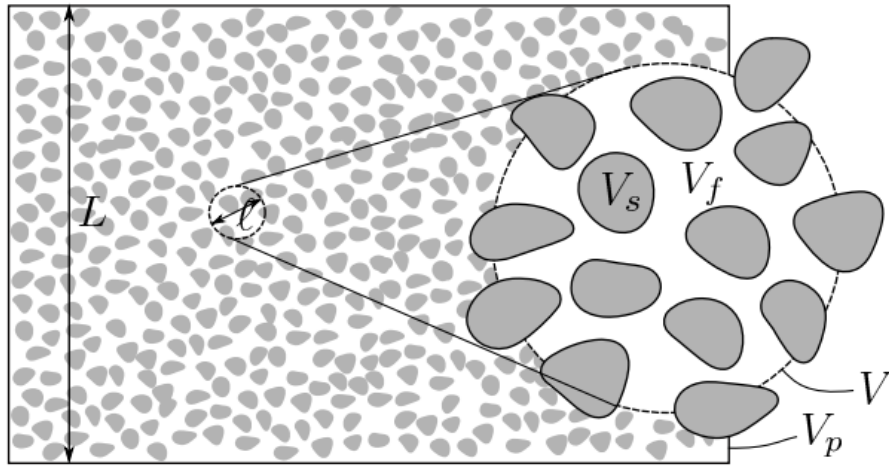


FIGURE 3.4: Illustration of volume averaging, with solid and fluid volumes V_s and V_f , respectively, in an arbitrary porous media [7]

As shown in figure 3.4, let V_p be the bulk volume of the porous media with L be the length scale. Consider $V \subset V_p$ represents the averaged volume with length scale l . V must be large enough to have statistical meaningful and small enough that $l \ll L$. In such case, an extrinsic volume-averaged quantity ψ_i can be defined as:

$$\langle \psi_i \rangle = \frac{1}{V} \int_{V_i} \psi_i dV \quad (3.29)$$

where $i \in \{f, s\}$ represents the phase where quantity ψ_i is described. Alternatively, intrinsic averaged can also be given as:

$$\langle \psi_i \rangle^i = \frac{1}{V_i} \int_{V_i} \psi_i dV \quad (3.30)$$

It is an average for a single phase only. These two types of averaged quantities are related to each other through porosity ($\phi = V_f/V$) as

$$\langle \psi_i \rangle = \begin{cases} \phi \langle \psi_f \rangle^f & \text{if } i = f \\ (1 - \phi) \langle \psi_s \rangle^s & \text{if } i = s \end{cases}$$

where ϕ is porosity.

The operators:

1. Gradient operator:

$$\langle \nabla \psi_i \rangle = \nabla \langle \psi_i \rangle + \frac{1}{V} \int_{A_{il}} \psi_i n_{il} dA \quad (3.31)$$

where $i, l \in \{f, s\}, i \neq l$ and n_{il} is the unit normal vector from i -phase to l -phase.

2. Divergence operator of a vector:

$$\langle \nabla \cdot a_i \rangle = \nabla \cdot \langle a_i \rangle + \frac{1}{V} \int_{A_{il}} a_i \cdot n_{il} dA \quad (3.32)$$

where a_i is a second-rank tensor.

3. Product operator:

$$\langle \psi_{i,1} \psi_{i,2} \rangle = \frac{1}{\phi_i} \langle \psi_{i,1} \rangle \langle \psi_{i,2} \rangle + \langle \tilde{\psi}_{i,1} \tilde{\psi}_{i,2} \rangle \quad (3.33)$$

where $\tilde{\psi}_{i,1}$ is pore-level spatial deviation, and $\psi_{i,1}$ is the intrinsic-volume average of quantity ψ_i .

3.4.1 Averaging of Mass Conservation Equation

Consider the flow to be incompressible in porous medium, the mass conservation equation 3.8 simplified into

$$\nabla \cdot v = 0 \quad (3.34)$$

Using divergence operator relation from 3.32, above equation 3.34 can be written in volume-averaged terms assuming constant porosity as:

$$\boxed{\nabla \cdot \langle v \rangle = 0} \quad (3.35)$$

The above equation 3.35 is the volume-averaged mass conservation equation.

3.4.2 Averaging of Momentum Conservation Equation

The incompressible flow momentum equation can be given by the NS equation:

$$\rho_f \left(\frac{\partial v}{\partial t} + v \cdot \nabla v \right) = -\nabla p + \mu_f \Delta v \quad (3.36)$$

where v represents the velocity vector, p is the pressure, ρ_f is the fluid density, and μ_f is the fluid's dynamic viscosity.

Averaged momentum equation can be given as follows:

$$\begin{aligned} \rho_f \left(\frac{\partial \langle v \rangle}{\partial t} + \frac{\langle v \rangle}{\phi} \cdot \nabla \langle v \rangle \right) &= -\phi \nabla \langle p \rangle^f + \mu_f \Delta \langle v \rangle \\ &+ \frac{1}{V} \int_{A_{fs}} (-\tilde{p} n_{fs} + \mu_f \nabla \tilde{v} \cdot n_{fs}) dA - \rho_f \nabla \cdot \langle \tilde{v} \tilde{v} \rangle \end{aligned} \quad (3.37)$$

where V is the volume of REV, ϕ is the porosity, and n_{fs} is the unit vector perpendicular to the fluid-solid interface

3.4.3 Averaging of Energy Conservation Equation

The governing equations at the pore scale for a porous media with fluid and solid phases can be given as follows:

$$\rho_f c_{pf} \left(\frac{\partial T_f}{\partial t} + v \cdot \nabla T_f \right) = k_f \Delta T_f \quad (3.38)$$

and

$$\rho_s c_s \frac{\partial T_s}{\partial t} = k_s \Delta T_s \quad (3.39)$$

where subscripts f and s are solid and fluid phases, respectively. The specific heat capacities are denoted as $c_{p,f}$ and c_s , respectively. k represents the thermal conductivities of the respective phase. Intrinsic volume-averaging these equations give:

$$\begin{aligned} \rho_f c_{p,f} \left[\phi \frac{\partial \langle T_f \rangle^f}{\partial t} + \langle v \rangle \cdot \nabla \langle T_f \rangle^f \right] &= \phi k_f \Delta \langle T_f \rangle^f + \nabla \cdot \left(\frac{1}{V} \int_{A_{fs}} k_f \tilde{T}_f n_{fs} dA \right) \\ &\quad + \frac{1}{V} \int_{A_{fs}} k_f \nabla \tilde{T}_f \cdot n_{fs} dA - \phi \rho_f c_{p,f} \nabla \cdot \langle \tilde{u} \tilde{T}_f \rangle^f \end{aligned} \quad (3.40)$$

and

$$\begin{aligned} (1 - \phi) \rho_s c_s \frac{\partial \langle T_s \rangle^s}{\partial t} &= (1 - \phi) k_s \Delta \langle T_s \rangle^s + \nabla \cdot \left(\frac{1}{V} \int_{A_{fs}} k_s \tilde{T}_s n_{sf} dA \right) \\ &\quad + \frac{1}{V} \int_A f_s k_s \nabla \tilde{T}_s \cdot n_{sf} dA \end{aligned} \quad (3.41)$$

Under the assumption of local thermal equilibrium between solid and liquid phases, temperature of the two phases have similar temperature, given as:

$$\langle T_f \rangle^f = \langle T_s \rangle^s = \langle T \rangle \quad (3.42)$$

Adding 3.40 and 3.41 gives zero as they are heat exchanges between one phase to other. Also, using 3.42 gives a semi-implicit closure relation represented by vafai et al. [37] as follows:

$$[\phi \rho_f c_{p,f} + (1 - \phi) \rho_s c_s] \frac{\partial \langle T \rangle}{\partial t} + \rho_f c_{p,f} \langle v \rangle \cdot \nabla \langle T \rangle = \nabla \cdot (k_e \cdot \nabla \langle T \rangle) \quad (3.43)$$

where k_e is the effective thermal conductivity tensor of the porous medium.

3.5 Summary of the Chapter

In this chapter 3, we started discussing about the flow within the porous media, followed by discussions on the models. Later, we discussed about the mathematical modelling of the flow through porous media. For this, we started with considering the assumptions made, forces which influence the fluid flow in porous matrix, and finally we derived the conservation equations for the fluid flow at micro-scale. We observed that there are different equations for the momentum equations, based on different assumptions and simplifications. In the last, we defined the volume averaging to derive the conservation equations at REV scale.

In the next chapter, we will discuss about the different models of evaporation from porous media.

Chapter 4

Evaporation through Porous Media

Evaporation from porous media is a crucial process with applications all around our life. It is vital from the engineering perspective also, with applications in wide engineering fields, such as drying of wood, cemented structures, textiles, drying of food-stuffs, and pharmaceutical products. Drying of the porous medium is widely used term in the daily life, which is a form of evaporation. Drying process is vital due to engineering applications. During the drying of porous media, interface between the free stream and porous media is crucial as there is complex interactions between the transport phenomena in porous media, medium properties and free stream.

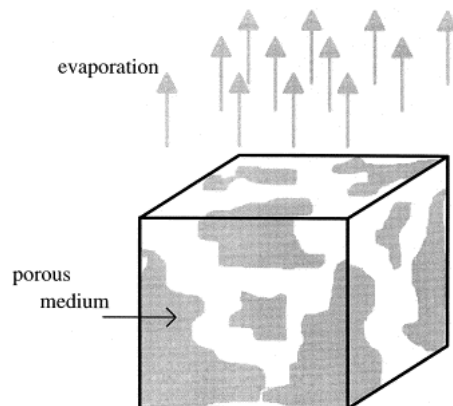


FIGURE 4.1: Illustration of evaporation from Porous Media [26]

The cause of evaporation can be factors such as convection of air, change of vapour pressure, relative humidity, temperature, heat transfer, and infrared radiation. In case of evaporation from porous media to ambient atmosphere, the evaporated fluid, which changed phase from liquid to gas, gets replaced with dry air and to maintain the saturation, porous media withdraws more liquid from layers from below where another end of the porous media is connected to the free liquid stream. For a completely saturated porous medium, early stage of the evaporation rate is relatively constant and high. Capillary actions lead to fluid flow from saturated zone towards the drying boundary. This flow happens along the hydraulically connected pathways through the interconnected pore networks [35, 27].

4.1 Drying Stages

Drying rates from a porous media strongly depend on the free flow conditions at the interface and flow regime. It is also dependent on the interconnected pore network

within the porous region. Drying from a porous medium is divided into different stages based on the rate of evaporation. A typical plot of the rate of evaporation from a porous medium versus time is shown in figure 4.2.

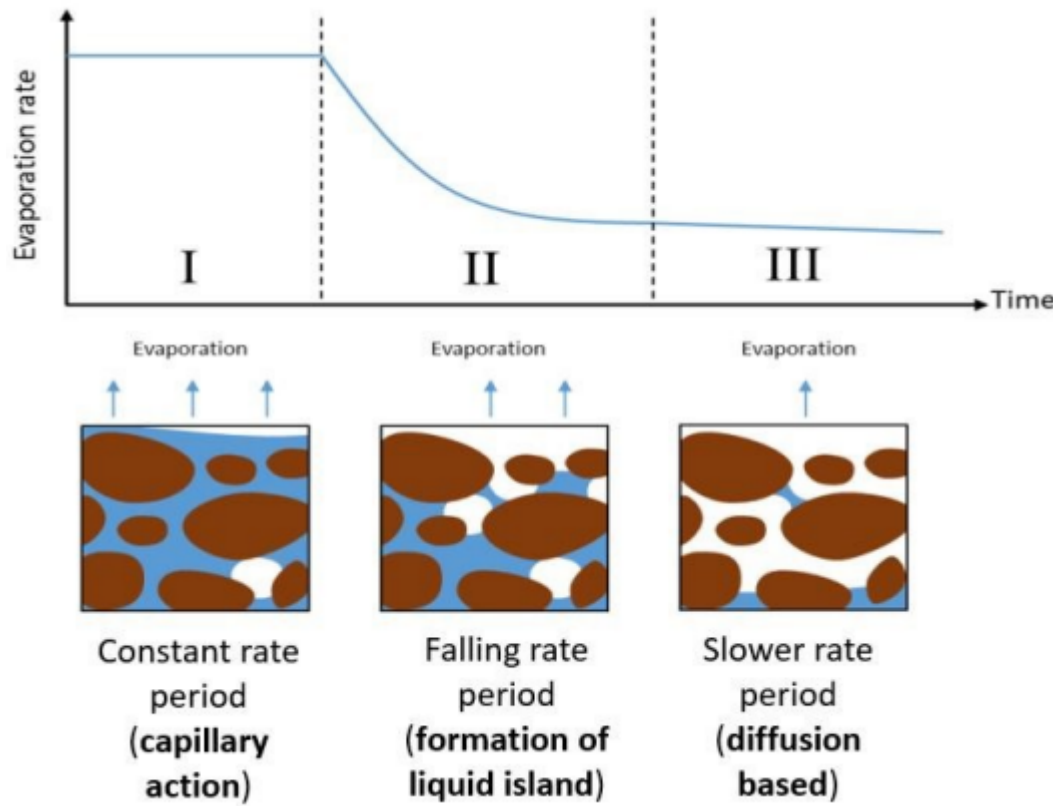


FIGURE 4.2: Qualitative illustration of different stages of drying rate from a porous media [7]

4.1.1 Stage-I

Stage 1 of the drying process is also called as constant rate rapid drying stage. During this stage, there is a continuous supply of the liquid phase within the porous media. The liquid phase is continuously supplied from the free liquid zone which is connected through the pore network. During this stage, capillary force dominates to transfer the liquid phase within the porous region to the surface. Due to continuous supply of the liquid to the saturated porous medium, the evaporation rate tends to be relatively high and remains almost constant.

4.1.2 Stage-IIa

Stage 2a is also called as falling rate drying stage. In this stage, the continuous liquid supply to the porous medium cuts off completely. In such case, liquid available within interconnected pore network only is transferred to the surface of porous medium by capillary effect. Due to no further supply of the free stream liquid, the capillary transfer rate to the surface of the porous medium reduces sharply, leading to drop in the evaporation rate.

4.1.3 Stage-IIb

Stage 2b is often referred to as the slow-evaporation or vapour-diffusion stage. In this stage, the capillary effect is unable to transfer the available liquids within the porous media to the interface. It is because the mass of liquid available within porous region is not enough to maintain connectivity. Hence, the liquid within porous region starts to evaporate due to partial pressure difference.

4.2 Review of Prior Models

Simultaneous heat and mass transfer from porous media carrying multi-phase fluid are coupled complexly. This complexity arises due to consideration of various effects such as gravity, capillarity and porous resistance.

Lewis [28] was the first among those, who tried to model the drying of the solids. He postulated that the drying of a porous solid consisted of two simultaneous processes. First, the liquid from the interior of solid moves to outer surface of the solid by diffusion, and second, the evaporation of liquids from the surface of the solids. The idea of diffusion was used by Sherwood [36] and he proposed a model for drying based on diffusion equation in the form

$$\frac{\partial S}{\partial t} = D \frac{\partial^2 S}{\partial t^2} \quad (4.1)$$

where S represents the saturation and D represents the diffusion coefficient. However, the work of Richards [33], who worked on the capillary actions in porous media. He suggested that only diffusion is not enough in deciding the flow, but capillarity also impact the flow in porous media significantly. Hence, the effect of surface tension cannot be neglected.

Hougen *et al.* [15], in their publication entitled "Limitations of Diffusion Equations in Drying", extensively made comparisons between the theoretical and experimental results based on the curves between capillary pressure and saturation. Van Arsdel [38] studied the effect of variable diffusivity in 1947 and published his finding in which he used a modified diffusion equation 4.1:

$$\frac{\partial S}{\partial t} = \frac{\partial}{\partial x} \left(D \frac{\partial S}{\partial t} \right) \quad (4.2)$$

where S denoted the saturation, and D represented diffusion coefficient.

Due to a variety of applications in engineering problems, modelling drying of porous media is vital. However, it is extremely complex as it involves various physical effects simultaneously. The motivation here is to present a modelling framework of coupled simulation of free stream and flow within a porous medium on the REV scale. The coupling concept has been introduced by [29], which is coupling the two domains at the interface.

In the pore space framework, many models and methods have been applied directly at micro scale by various researchers. Kazemian *et.al.* [20] used direct numerical simulation (DNS) and lattice-Boltzmann method (LBM) to characterize the evaporation at pore scale. Wilson *et.al.* utilized the volume-of-fluids (VoF) method to describe the multi-phase effects on evaporation in porous media. The same governing equations are applicable in both free flow and porous medium in such cases. Hence, no mechanism is needed for the coupling of free air stream and porous medium at the interface.

At the REV scale, these models are no more applicable in the porous medium, but they can still be employed in the free stream. At the REV scale, the fluid flow in porous media is governed by the Darcy-Forchheimer equation 5.1. In two sub-domains, two different governing equations are applicable. These two governing equations require coupling for the connectivity.

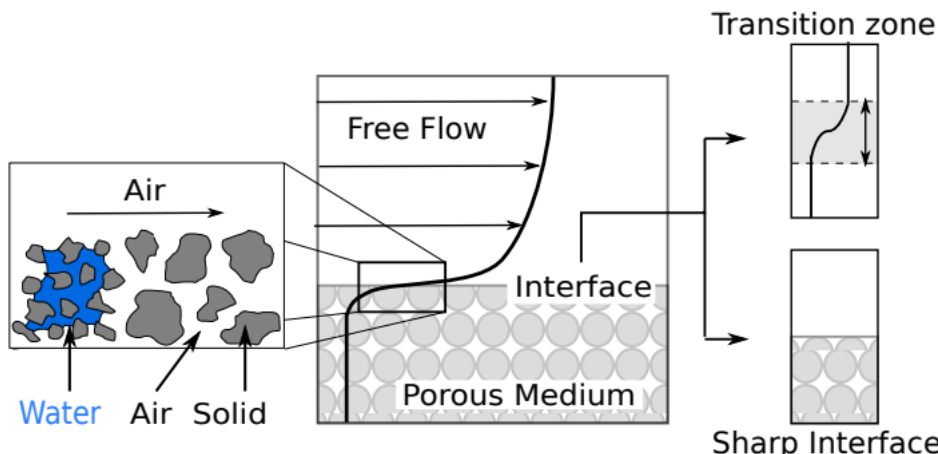


FIGURE 4.3: Description of Coupling at Interface [29]

For such coupling on REV scale, various strategies have been introduced. However, single-domain and two-domain approaches introduced by [19] are quite popular coupling methods.

4.2.1 Single-Domain Coupling Model

Free flow zone	$\phi = 1$ $K \gg 1$
$-\nabla \cdot (\mu \nabla v) + \mu K^{-1} v + \nabla p = f$ $\nabla \cdot v = 0$	
Transition zone	
$-\nabla \cdot (\mu \nabla v) + \mu K^{-1} v + \nabla p = f$ $\nabla \cdot v = 0$	
Porous zone	$\phi < 1$ $K \ll 1$

FIGURE 4.4: Single domain approach using Brinkman equation with a transition zone

The single-domain approach is based on a single set of equations valid throughout the fluid domain in both the free flow and porous regions as shown in figure 4.4. Brinkman [4] worked on a single coupled equation, a combination of Darcy's equation and (Navier-)Stokes equation, and can be applied to entire domain. In such case, equation 3.37 can be written on REV scale as:

$$-\nabla \cdot (\mu_{eff} v) + \frac{\mu_f}{K} v + \nabla p = f \quad (4.3)$$

where μ_f is fluid viscosity, μ_{eff} is effective viscosity, f is external force, and K is permeability of the porous domain.

This approach involves transitioning from one domain to another through a transition zone at the interface between the porous medium and the free-flow zone. In this zone, the porous properties are continuously vary instead of allowing a discontinuous jump. Due to changes in parameters in the transition region, the quantities like pressure, velocity, and temperature vary enormously. Since same equations are applicable throughout the subdomains, the flux and stress continuity are satisfied and do not require unique coupling at the interface. However, momentum continuity is not satisfied. Hence, to compensate for it, *effective viscosity* μ_{eff} has been introduced which accounts for momentum exchange in the transition zone. The effective viscosity depends strongly on the fluid types in free flow and porous medium, the direction of flow as well as geometric properties of the porous medium.

The diffusion term in the porous region is negligible due to slow (creeping) flow. Similarly, in the free flow zone, permeability $K \rightarrow \infty$ which implies that $pK^{-1}v \rightarrow 0$ and can be ignored.

4.2.2 Two-Domain Coupling Model

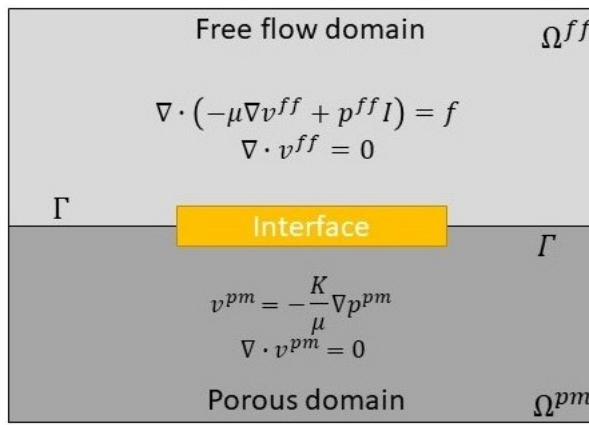


FIGURE 4.5: Two-Domain coupling approach with sharp interface and strong coupling condition

Contrary to the single-domain approach, there are two separate domains in the *two-domain approach*. One corresponds to free flow, and other to the porous medium with a sharp interface. Since both domains are separate, they are governed by different equations. The porous region flow is governed by Darcy-Forchheimer equation

[3.16](#), while the free flow is governed by (Navier-)Stokes equation [3.21](#). It also requires a strong coupling between both distinct subdomains. The coupling should be robust enough to integrate relevant quantities through the interface from free flow to REV-scaled porous medium and vice-versa so that proper transfer of information can be guaranteed from one to another.

Various ways have been given forward to derive the coupling conditions. However, the most robust is based on the volume-averaging technique given by [\[12\]](#) and [\[39\]](#).

4.2.3 Evaporation Models on REV

On the REV scale, the modelling of the evaporation is done through the decoupled models. Either they focused more on the decoupled flows or the porous medium. Furthermore, the adsorption or advection of the free flow fluid to the porous medium is often neglected to simplify the complexity of the coupled equations. They are primarily based on Richard's equation [\[33\]](#) in the extended form. Few presented models in the next section include the coupled heat and mass transfer equations considering the phase change.

4.3 Mathematical Modelling of Coupled Evaporation

Modelling coupled equation for the simultaneous heat and mass transfer through porous media along with the phase change is highly complex. Various coupled models have been put forward based on the assumptions on the pore and REV scales.

4.3.1 Bouddour Model [\[3\]](#)

At the pore scale, the homogenization method is to be incorporated here for porous media in terms of *Representative Elementary Volume (REV)*. This REV is small compared to the macroscopic volume, which is in consideration. In periodic media, the period size equals REV. It can be represented in terms of characteristic length l and characteristic dimension L . The separation of scales parameter ϵ is introduced as scaling factor. ϵ represents a value which is small enough compared to the total length of the porous media, but should be large enough with respect to microscopic scale. It can be given as follows:

$$\epsilon = \frac{l}{L} \ll 1 \quad (4.4)$$

It satisfies the condition that macroscopic models depend on phenomena and internal characteristics of porous media as well as independence from boundary conditions of the porous medium. Different researchers used different values to represent ϵ depending on the problems they were studying.

Governing equation for vapour mass fraction ω_v at pore scale can be given as follows:

$$\rho_g \frac{\partial \omega_v}{\omega t} + \rho_g v_g \frac{\partial \omega_v}{\partial x} - \frac{\partial}{\partial x} \left(\rho_g D \frac{\partial \omega_v}{\partial x} \right) = 0 \quad (4.5)$$

where ρ_g is mass density, v_g is velocity of gas, and D is the binary air-vapour diffusion coefficient. Also, the velocity of the air-vapour mixture can be written as

$$v_g = \omega_v v_v + \omega_a v_a \quad (4.6)$$

where subscripts v and a stand for vapour and air respectively.

Heat transfer can be described in liquid and gaseous phases by the following micro-scale equation

$$(\rho c_p)_\beta \frac{\partial T_\beta}{\partial t} + (\rho c_p)_\beta v_\beta \frac{\partial T_\beta}{\partial x} - \frac{\partial}{\partial x} \left(\lambda_\beta \frac{\partial T_\beta}{\partial x} \right) = 0 \quad (4.7)$$

where β is the phase, T_β is the temperature, v_β is the velocity of similar phase. However, heat transfer in the solid phase can be governed by conduction and can be expressed as

$$(\rho c_p)_s \frac{\partial T_s}{\partial t} - \frac{\partial}{\partial x} \left(\lambda_s \frac{\partial T_s}{\partial x} \right) = 0 \quad (4.8)$$

where subscript s represents the solid medium, c_p is heat capacity, and λ is the thermal conductivity of the solid phase.

The proper boundary conditions can be resolved on Γ_{gl} , Γ_{gs} and Γ_{ls} . The conditions on the liquid-gas interface, assuming insolubility, can be given as

$$v_a n^g = 0 \text{ on } \Gamma_{gl} \quad (4.9)$$

where n^g represents the outward normal unit.

The continuity equation for the vapour flux can be written as

$$\rho_a v_p N^g = -\rho_g D \frac{\partial \omega_v}{\partial x} N^g \text{ on } \Gamma_{gl} \quad (4.10)$$

And mass conservation on Γ_{gl} can be represented as

$$\rho_l (v_l - \omega) N^g = \rho_g (v_p - \omega) N^g \quad (4.11)$$

Similarly, on the solid-gas interface Γ_{gs} , the boundary conditions can be given as

$$\rho_g D \frac{\partial \omega_v}{\partial x} N^g = 0 \quad (4.12)$$

$$T_g = T_s \quad (4.13)$$

$$\lambda_g \frac{\partial T_g}{\partial x} N^g = \lambda_s \frac{\partial T_s}{\partial x} N^g \quad (4.14)$$

And, on liquid-solid interface Γ_{ls} , boundary conditions are

$$T_l = T_s \quad (4.15)$$

$$\lambda_l \frac{\partial T_l}{\partial x} N^l = \lambda_s \frac{\partial T_s}{\partial x} N^l \quad (4.16)$$

4.3.2 Zhang Model [41]

The model presented by Zhang *et al.* [41] is based on the theories combining Luikov's model with Whitaker's model proposed by Ilic [17], who described the evolution of

temperature, pressure and vapour distributions in both dry and wet regions. It is based on continuum-based approach. The theory used the irreversibility theory of thermodynamics to derive a coupled-field model. Volume averaging the coupled-field models, a complete theoretical framework for describing the flow and heat transfer in porous media was devised for the convective drying of porous media.

Porous materials can be classified into two types: wettable and non-wettable. Depending upon the types of porous media which provide continuous or discontinuous wet patches, the drying period varies. It can be divided into different drying periods as

1. Constant rate drying period

Suppose initially, liquid content of the porous media is high enough. In such case, the surface of the porous media is covered with a continuous layer of free liquids and evaporation occurs mainly at the surface. The movement of the fluid is not only maintained by capillary force but also driven by many other forces including liquid-solid matrix interfacial drag, inertial force, gravity etc. In such conditions, internal liquid transfer to the surface and evaporation from the porous media surface is in equilibrium. Thus, a constant drying rate observes during such equilibrium. If the temperature of the porous material is negligible, the surface temperature is almost constant.

2. First falling rate period

As drying continues, the fraction of wet area at the surface decreases with decreasing surface liquid content. When the free liquid content in the porous media is greater than the saturation, the liquid phase is continuous. But, when it decreases below saturation liquid content, the surface will form discontinuous wet patches based on the randomly distributed paths. Thus, the mass transfer coefficient decreases with the surface free liquid content, showing the first falling rate period. In this case, Clapeyron equation determines the vapour pressure. At such conditions, convective and heat transfer coefficients at the surface are the function of surface liquid content which gives the relationship as

$$h_o = h_{o,0} \left[\eta_h + (1 - \eta_h) \frac{\epsilon_l - \epsilon_{l,ir}}{\epsilon_{l,c} - \epsilon_{l,ir}} \right] \quad (4.17)$$

$$h_m = h_{m,0} \left[\eta_m + (1 - \eta_m) \frac{\epsilon_l - \epsilon_{l,ir}}{\epsilon_{l,c} - \epsilon_{l,ir}} \right] \quad (4.18)$$

where $\epsilon_{l,c}$ is the saturated liquid content, $\epsilon_{l,ir}$ is the maximum irreducible liquid content, and η_h and η_m are constants determined experimentally.

3. Second falling rate period

When the surface liquid content reaches the maximum sorptive value after further drying, drying patches appear. There is no free liquid on the surface. At such conditions, the surface temperature increases rapidly, which is the start of second falling rate. In this case, the system is divided into two regions, one is wet region and another is dry region. In such cases, the movement of liquid happens inside only the wet region, and capillary action is main driving force. The driving force behind this capillary action is vapour pressure gradient, and can be given as

$$J_b = -\rho_l D_b \nabla \epsilon_l \quad (4.19)$$

where J_b is liquid flux and k_b is the permeability of the liquid phase, D_b is defined as liquid phase conductivity and can be given by Arrhenius-type function of temperature as

$$D_b = D_{b,0} \left(\frac{\epsilon_{l,b} - \epsilon_{l,eq}}{\epsilon_{l,tr} - \epsilon_{l,eq}} \right)^3 \exp\left(-\frac{E_a}{RT}\right) \quad (4.20)$$

where $\epsilon_{l,eq}$ is equilibrium liquid content, E_a is defined as transfer activation energy of liquid phase.

Drying Models

Based on above analysis, following mathematical model is established to describe heat and mass transfer during constant rate and falling rate periods in convective drying of porous media.

1. Wet Region Model

Mass conservation equations :

Liquid phase:

$$\frac{\partial(\rho_l \epsilon_l)}{\partial t} + \nabla \cdot (\rho_l \vec{v}_l) = -\dot{m} \quad (4.21)$$

Gas phase:

$$\frac{\partial(\rho_g \epsilon_g)}{\partial t} + \nabla \cdot (\rho_g \vec{v}_g) = \dot{m} \quad (4.22)$$

Air:

$$\frac{\partial(\rho_a \epsilon_g)}{\partial t} + \nabla \cdot (\rho_a \vec{v}_g - \rho_v \vec{v}'_v) = 0 \quad (4.23)$$

Vapour:

$$\frac{\partial(\rho_g \epsilon_g)}{\partial t} + \nabla \cdot [\rho_v (v'_v + v'_g)] = 0 \quad (4.24)$$

where \dot{m} is evaporation rate and v'_v is vapour diffusion velocity.

Momentum equation :

Gas phase:

$$\frac{\partial v_g}{\partial t} + v_g \cdot \nabla v_g - \frac{\dot{m} v_g}{\rho_g} = -\frac{1}{\rho_g} \nabla p_g - \epsilon_g g + v_g \nabla^2 v_g - \frac{v_g \epsilon_g}{k k'_g} v_g \quad (4.25)$$

Liquid phase:

$$\frac{\partial v_l}{\partial t} + v_l \cdot \nabla v_l - \frac{\dot{m} v_l}{\rho_l} = -\frac{1}{\rho_l} \nabla p_l - \epsilon_l g + v_l \nabla^2 v_l - \frac{v_g \epsilon_l}{k k'_l} v_l \quad (4.26)$$

Vapour diffusion equation:

$$v'_v = -\epsilon_g D_{va} \frac{P}{P - P_v} \cdot \frac{1}{\rho_v} \nabla \rho_v \quad (4.27)$$

Energy Equation :

$$(\epsilon_s \rho_s c_s + \epsilon_l \rho_l c_l + \epsilon_g \rho_g c_g) \frac{\partial T}{\partial t} + (\rho_l c_l v_l + \rho_a c_a v_a + \rho_v c_v v_v) \cdot \nabla T + \gamma \dot{m} = \nabla \cdot [(\lambda_m + \rho_l c_l D_d) \nabla T] \quad (4.28)$$

2. Dry Region Model

Mass conservation equation :

Liquid phase:

$$\frac{\partial(\rho_l \epsilon_b)}{\partial t} + \nabla \cdot (\rho_l v_b) = -\dot{m}_b \quad (4.29)$$

Air:

$$\frac{\partial(\rho_a \epsilon_g)}{\partial t} + \nabla \cdot (\rho_a v_g - \rho_v v'_v) = 0 \quad (4.30)$$

Vapour:

$$\frac{\partial(\rho_g \epsilon_g)}{\partial t} + \nabla \cdot (\rho_v (v'_v + v_g)) = \dot{m}_b \quad (4.31)$$

where subscript b represents the liquid phase in porous media.

Momentum equation :

Gas phase:

$$\frac{\partial v_g}{\partial t} + v_g \cdot \nabla v_g + \frac{\dot{m} v_g}{\rho_g} = -\frac{1}{\rho_g} \nabla p_g - \epsilon_g g + v_b \nabla^2 v_g - \frac{v_g \epsilon_g}{k k'_g} v_g \quad (4.32)$$

Liquid phase:

$$v_b = -D_b \nabla \epsilon_b \quad (4.33)$$

Energy equation :

$$(\epsilon_s \rho_s c_s + \epsilon_b \rho_b c_b + \epsilon_g \rho_g c_g) \frac{\partial T}{\partial t} + (\rho_b c_b v_b + \rho_a c_a v_a + \rho_v c_v v_v) \cdot \nabla T + \gamma \dot{m}_b = \nabla \cdot [\lambda_m \nabla T] \quad (4.34)$$

4.4 Summary of the Chapter

In this chapter 4, we discussed in details about the coupled models for the evaporation in porous media. We discussed about different stages involved in the evaporation process. There are two different regions. In the first stage, evaporation rate is relatively fast and constant. In the second stage, first rate of evaporation falls rapidly and becomes constant and slow after some time. We also looked into some models developed in earlier days of theoretical developments, where we talked about the Sherwood model 4.1 and Van Arsdel model 4.2. Since these equations didn't consider the capillary effects and only diffusion effects. Richards [33] gave a new formulation with capillary effects. Afterwards, we looked into coupling models, single-domain coupling and two-domain coupling. Here, we talked about the need of the coupling between the free flow and porous media flow. We introduced the transition zone concept for the single-domain coupling. We discussed in details about the coupled evaporation models on the REV by the Bouddour [3] and Zhang [41].

In the next chapter, we will discuss about the numerical methods and tools used for this thesis.

Chapter 5

Numerical Modelling

5.1 OpenFOAM

OpenFOAM (Open Source Field Operation and Manipulation) is an open-source collection of C++ libraries for solving the PDEs numerically, specifically used to solve Computational Fluid Dynamics (CFD) problems numerically. OpenFoam is a cell-centered finite volume method (FVM) solver for Computational Fluid Dynamics (CFD), which supports unstructured arbitrary shaped meshes. It consists of a bundle of libraries and codes which can solve highly complex physical phenomena such as turbulence, electromagnetics, chemical reactions, and combustion.

It is written in object-oriented C++ and is open-source. It allows users to control and modify the source code, controlling the solution of the CFD problems. In this thesis, *porousEvapFoam* solver is used, developed by Dr Bahram Haddadi (TU Wien). OF9 has been used in this study.

5.2 porousEvapFoam: An OpenFOAM Solver

porousEvapFoam is an OpenFOAM solver capable of solving the evaporation problems in a porous media due to heating (boiling evaporation based solver). This solver is also capable to problems involving multiphase liquids and their evaporation. It is based on *chtMultiRegionFoam*, which also considers the coupling of different regions with different physics. Currently, *porousEvapFoam* is only capable of solving incompressible flows. Supported momentum transport models are laminar, RAS and LES. There is coupling between porous region to solid region, porous region to fluid region, and coupling between fluid region to solid region.

Figure 5.1 shows the flowchart of the evaporation process in the solver. Figure 5.2 shows the structure of the porousEvapFoam solver.

5.2.1 Momentum Conservation Model

porousEvapFoam is based on a single-domain coupling model, as mentioned in 4.2.1. It couples the porous medium to the free flow region through *Darcy-Forchheimer-Stokes equation*. Compared to equation 4.3, which is only applicable for creeping flow, the *Darcy-Forchheimer-Stokes equation* can be extended easily for the higher Reynolds number and in turbulent conditions [1]. The model equation can be given as follows:

$$\frac{\partial \rho v}{\partial t} + \nabla \cdot (\rho v v) = -\nabla p + \nabla^2 v + S_m \quad (5.1)$$

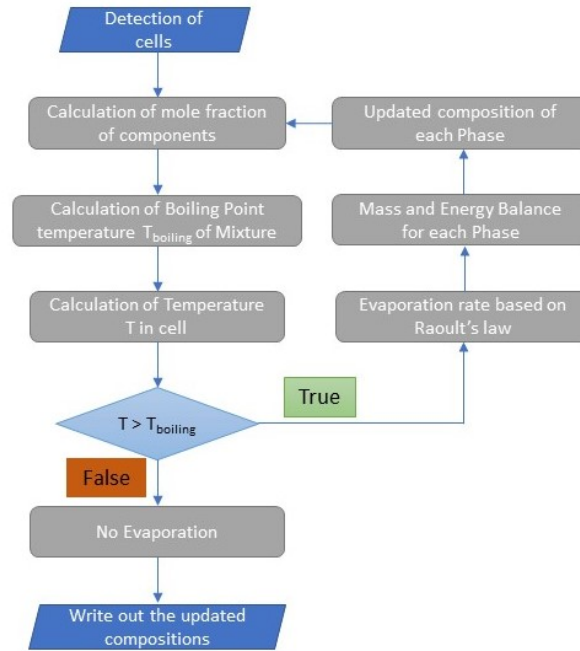


FIGURE 5.1: Flowchart of Evaporation in porousEvapFoam solver

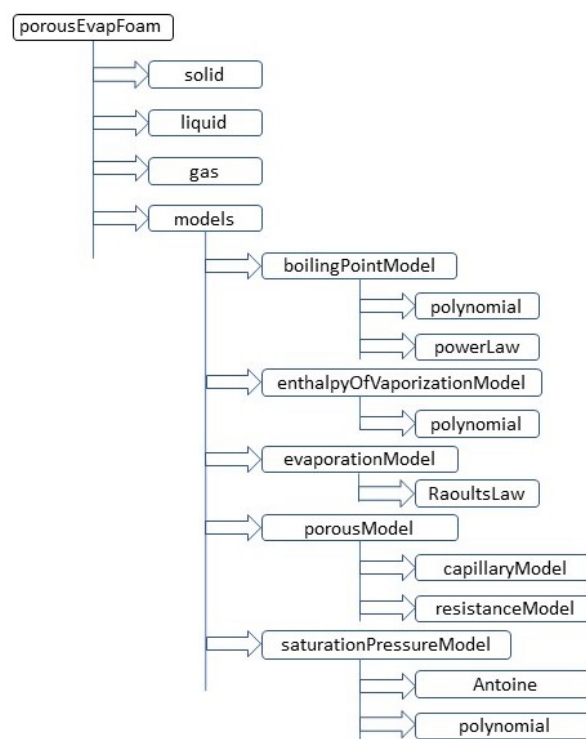


FIGURE 5.2: Structure of porousEvapFoam Solver

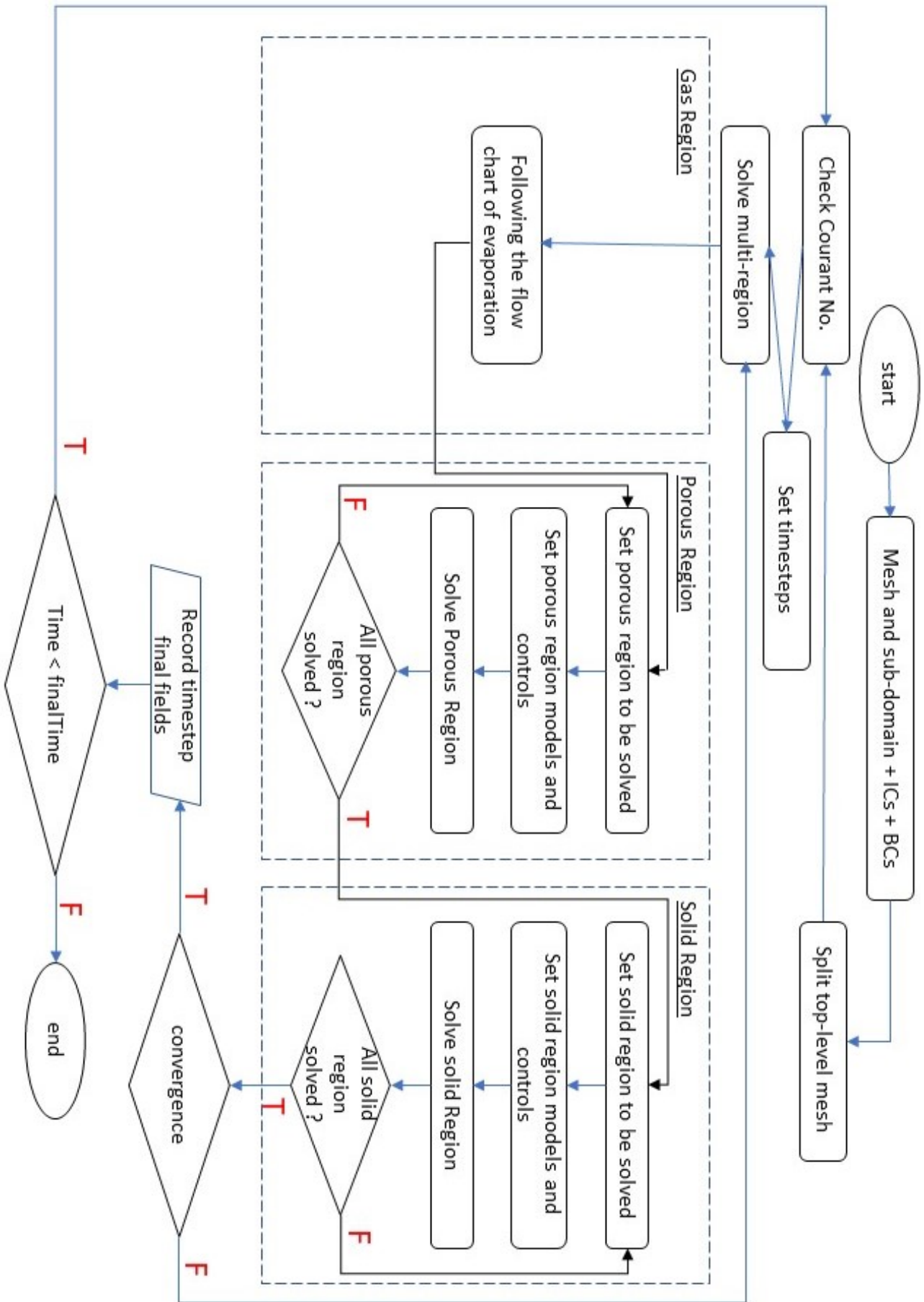


FIGURE 5.3: Overall flowchart of porousEvapFoam solver for multi-region

where S_m acts as a sink term originates due to porous resistance and can be given by

$$S_m = \left(\mu D + \frac{1}{2} \rho t r(v \cdot T) F \right) v \quad (5.2)$$

where F and D are coefficients which are needed to be modelled based on the porous media properties.

Calculation of Coefficients

The coefficients of equation 5.2 are needed to be estimated for the solution of the momentum equation. Hence, we need to consider that pressure is a function of velocity in the porous media and can be expressed as $p(U)$. Now, equation 5.2 can be rewritten as:

$$S_m = \mu D v + \frac{1}{2} \rho t r(v \cdot I) F v \quad (5.3)$$

and S_m is supposed to be equal to ∇p , which gives:

$$\nabla p = \mu D v + \frac{1}{2} \rho t r(v \cdot I) F v \quad (5.4)$$

In the cartesian coordinate system, it can be written as:

$$\nabla p = \mu D_i v_i + \frac{1}{2} F_i |v_j| v_i \quad (5.5)$$

Considering pressure to be a polynomial function of velocity, it is given as:

$$\nabla p = \frac{\Delta p}{\Delta x} = A v + B v^2 \quad (5.6)$$

Comparing equations 5.5 and 5.6, we get

$$A = \mu D \quad (5.7)$$

$$B = \frac{1}{2} \rho F \quad (5.8)$$

Hence, coefficients D and F can be calculated based on values of A and B , which are derived from the pressure and velocity correlation in the media.

5.2.2 PIMPLE Algorithm

The PIMPLE algorithm combines the SIMPLE (an acronym for *Semi-Implicit Method for Pressure-Linked Equations*) and PISO (an acronym for *Pressure-Implicit with Splitting of Operators*) algorithms. In this algorithm, a specified number of correction loops are performed while seeking a steady-state solution that converges, followed by solving other transport equations afterwards. The PIMPLE algorithm gives more flexible control to use a higher *Courant number* (Co) (> 1), which allows for greater time steps while simulating [31].

As shown in figure 5.4, the PIMPLE algorithm consists of two iterations. They are *inner iteration* and *outer iteration*. The inner iteration is performed over Poisson's problem, which is ill-posed. This pressure value is used to calculate intermediate pressure and velocities iteratively, while outer iterations modify and update the velocity matrix in the momentum equations. In OpenFOAM, these can be done as follows:

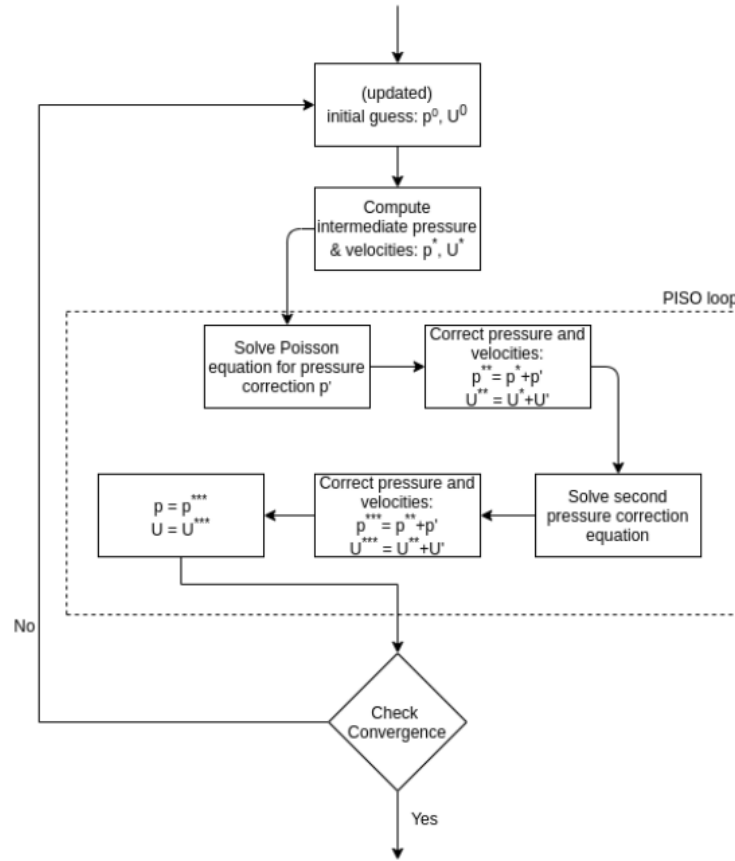


FIGURE 5.4: Flowchart for PIMPLE Algorithm [31]

- *nCorrectors*: It refers to inner iterations.
- *nOuterCorrectors*: It refers to outer iteration.

5.2.3 Courant Number

In the context of numerical simulation and stability, the Courant Number is one of the critical parameters. It regulates the transport of the information in the CFD simulations. The CFL (Courant-Friedrichs-Lowy) condition is an essential criterion for the convergence of the solution of the PDEs. It arises from the explicit time discretization in the numerical integration.

For the n-dimensional case, it can be given as:

$$C = \Delta t \left(\sum_{i=1}^n \frac{v_{x_i}}{\Delta x_i} \right) \leq C_{max} \quad (5.9)$$

where C is the Courant number, C_{max} is the maximum Courant number, Δx is the spatial step, Δt is time steps, and v_i is flow velocity.

5.3 Discretization of Momentum Equation

The momentum equation for flow in porous media given in equation 5.1 can be written in integral form as:

$$\underbrace{\int_{\Omega} \frac{\partial \rho v}{\partial t} d\Omega}_{\text{Temporal}} + \underbrace{\int_{\Omega} \nabla \cdot \rho v v d\Omega}_{\text{Convection}} = - \underbrace{\int_{\Omega} \nabla p d\Omega}_{\text{Pressure}} + \underbrace{\int_{\Omega} \nabla \cdot (\nabla v) d\Omega}_{\text{Diffusion}} + \underbrace{\int_{\Omega} S_m d\Omega}_{\text{Sink}} \quad (5.10)$$

where S_m is the sink term that arises due to porous media resistance and Ω is the volume of the domain.

To solve the momentum equation numerically through the finite volume method, the first step is to discretize the momentum equation from the integral form to the algebraic form. Discretization of individual terms are given as follows:

5.3.1 Temporal Term

Considering an arbitrary function Ψ which is a function of t as $\Psi(t)$. By Taylor's expansion rule, it can be given as follows:

$$\Psi(t + \Delta t) = \Psi(t) + \Delta t \left(\frac{\partial \Psi}{\partial t} \right) + (\Delta t)^2 \left(\frac{\partial^2 \Psi}{\partial t^2} \right) + \dots \quad (5.11)$$

First-order accurate linear expansion can be given as:

$$\Psi(t + \Delta t) = \Psi(t) + \Delta t \left(\frac{\partial \Psi}{\partial t} \right) \quad (5.12)$$

Using the above relation 5.12 on the temporal term in the momentum transport equation with parameters $\rho(t)$ and $v(t)$:

$$\int_{\Omega} \frac{\partial \rho v}{\partial t} d\Omega \approx \frac{\rho^{n+1} v^{n+1} - \rho^n v^n}{\Delta t} \quad (5.13)$$

5.3.2 Convection Term

Using Gauß divergence theorem, a volume integral can be reduced into a surface integral. Using this theorem on the convection term:

$$\int_{\Omega} \nabla \cdot (\rho v v) d\Omega = \int_{\Gamma} (\rho v v) \cdot n ds \quad (5.14)$$

where n is the normal unit vector, and Γ is the closed surface.

Replacing the surface integral with summation over neighbouring cell faces gives:

$$\int_{\Gamma} (\rho v v) \cdot n ds \approx \sum_{face} \Gamma \cdot (\rho v)_f v_f = \sum_{face} F v_f \quad (5.15)$$

where Γ is the surface area, and F is flux through the face, defined as $F = \Gamma \cdot (\rho v)_f$.

5.3.3 Pressure Term

The pressure term in equation 5.10 is given as:

$$\int_{\Omega} \nabla p d\Omega = \oint_{\Gamma} p \cdot n ds = \sum_{face} S \cdot p_f \quad (5.16)$$

where p_f is interpolated stress term at face centres in a collocated grid.

5.3.4 Diffusion Term

The diffusion term is discretized in the similar manner as the convection term.

$$\int_{\Omega} \nabla \cdot (\nabla v) d\Omega = \oint_{\Gamma} (\nabla v) \cdot n ds \approx \sum_{face} (\nabla_f v) \cdot S \quad (5.17)$$

Here ∇_f is the face gradient.

5.3.5 Sink Term

The sink term arose in the porous media flow due to the resistance of the porous effect and was added as the Darcy-Forchheimer coefficients. It can be directly integrated over the control volume as S_m is calculated explicitly through equation 5.2.

Hence, the discretized momentum equation 5.10 can be expressed in the algebraic form as

$$a_p u_p + \sum_N a_N u_N = -\nabla p + S \quad (5.18)$$

where subscript p represents the current node in the control volume while subscript N represents the neighbouring cells and their values.

The above equation can be further simplified as

$$a_p u_p = H(u) - \nabla p \quad (5.19)$$

$$u_p = \frac{H(u)}{a_p} - \frac{\nabla p}{a_p} \quad (5.20)$$

which is in the form

$$[A][u] = [B] \quad (5.21)$$

To solve the algebraic equation 5.21, OpenFOAM offers different solvers depending on the choice of discretization method. In the next section, we will look into different numerical schemes and solvers available in OpenFOAM.

5.4 Numerical Schemes

OpenFOAM has a wide range of discretization schemes for different terms originating from complex PDEs such as Navier Stokes. The discretization schemes are mentioned in *fvSchemes* within the *system* directory in OpenFoam. A short description of available discretization schemes is mentioned below:

5.4.1 Time Schemes

The time schemes define how a property is integrated as a function of time:

$$\frac{\partial}{\partial t}(\Psi) \quad (5.22)$$

Depending on the choice of the discretization scheme, values at older time steps are needed, which can be represented as Ψ^0 for 1-step older and Ψ^{00} for 2-step older values.

Popular *ddtSchemes* are mentioned in table 5.1.

ddtSchemes	Details
Euler Implicit	Implicit, first order and transient
Crank-Nicolson	Second Order, transient, and bounded
steadyState	Steady-state, set temporal derivative to 0

TABLE 5.1: OpenFoam Schemes for time discretization

5.4.2 Gradient Schemes

Different gradient schemes are available in the OpenFOAM packages. It is usually available in the syntax:

<optional limiter> <gradient scheme> <interpolation scheme> (5.23)

Some of the important *gradSchemes* are given in the table 5.2 below.

gradSchemes	Details
leastSquares	Second order and least squared
Gauß<interpolation scheme>	Second Order, Gauß integration

TABLE 5.2: OpenFoam Schemes for gradient

5.4.3 Divergence Scheme

The default scheme for divergence in OpenFoam is Gauss divergence scheme. However, there are many more interpolation schemes available in the package. It is usually available in the syntax:

Gauß <interpolation scheme> (5.24)

Most used interpolation schemes for the divergence are given below in table 5.3.

divSchemes	Details
linear	Second order and unbounded
upwind	First order and bounded
QUICK	Second order and bounded

TABLE 5.3: OpenFoam Interpolation schemes for divergence

5.4.4 Laplacian Schemes

Laplacian terms are pretty standard in CFD problems, which refer to diffusion. Taking the laplacian of the term Ψ , it can be written as:

$$\nabla^2 \Psi = \nabla \cdot (\alpha \nabla \Psi) \quad (5.25)$$

where α represents the diffusion coefficient.

It is usually given in the syntax in OpenFoam as

```
Gauß <interpolation scheme> <snGradScheme> \quad (5.26)
```

Usual interpolation schemes for the laplacian scheme are represented in the table 5.3. Popular choices for *snGradScheme* are:

- corrected
- uncorrected
- limited

5.5 Simulation Case Setup

To have a better understanding of the evaporation from porous media to free-flow, a general case has been studied. We will see the detailed simulation setup in the OpenFOAM in this section.

5.5.1 Geometry Setup

A sample geometry is constructed as shown in figure 5.5. The geometry consists of a heater, porous, and free-flow regions as shown. The calculated Reynolds number is 1600. The free stream velocity is 10 m/s through the free flow region.

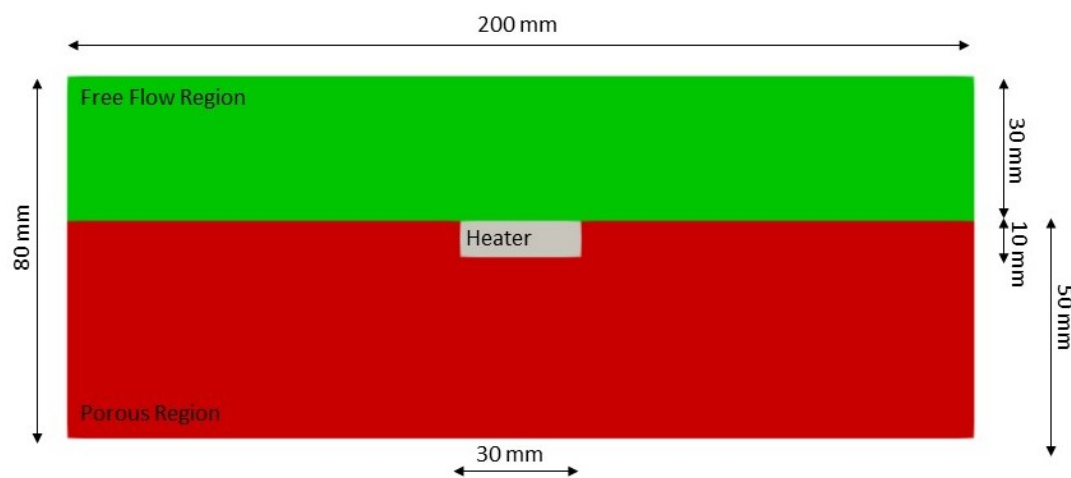


FIGURE 5.5: Front View of the sample Geometry

The overall geometry is shaped like a box of dimensions 200 mm x 80 mm x 200 mm. In figure 5.5, it can be seen that the green region is free-flow region, the grey region is the heater and the red region is the porous medium saturated with binary liquids with equal proportions.

5.5.2 Mesh

Since the structure of the geometry is basic, OpenFOAM's *blockMesh* utility has been utilized for the generation of the mesh. The *blockMesh* can create a good quality mesh for the basic 3-dimensional geometry. For the lower computational costs, the mesh is kept as coarse as it is possible for the study. Different regions have been named differently for the study purpose and simplification while mentioning boundary conditions. The porous region has been named *porous*, the heater region has been renamed *heater* and the free-flow region is renamed *fluidDomain*. The meshed region is shown in figure 5.6.

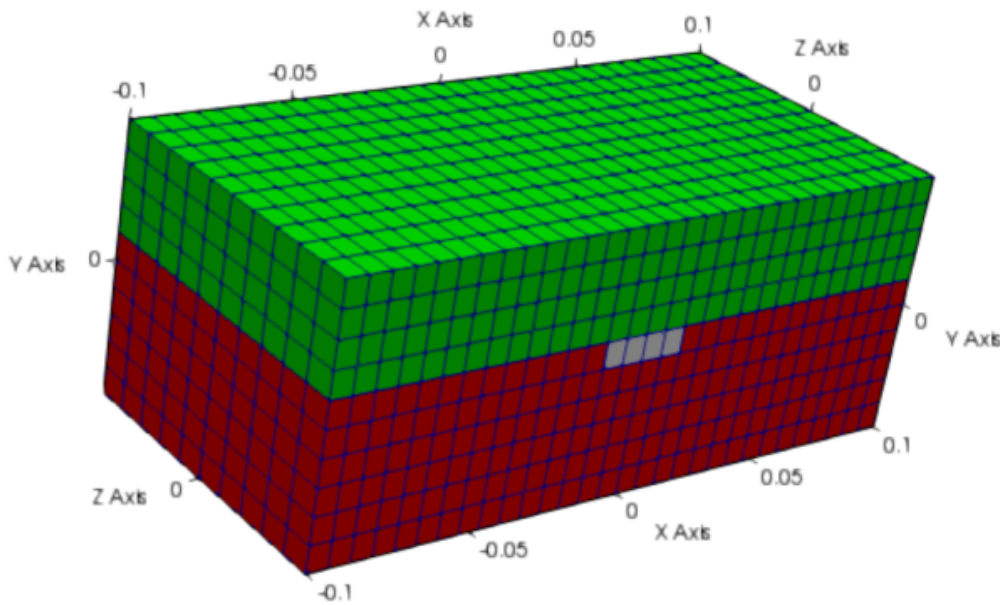


FIGURE 5.6: Mesh of the geometry generated using *blockMesh*

The mesh generated is of high quality and consists of total 3000 cells. Since the Reynolds Number ($Re < 2000$) corresponds to the laminar flow regime, we do not add prism layers. The region-wise cells can be seen in table 5.4.

Region	Number of Cells
fluidDomain	1200
heater	40
porous	1760

TABLE 5.4: Number of cells in each region

To generate different mesh regions, *topoSet* OpenFOAM's utility has been used, which can assign different regions in a single mesh domain.

5.5.3 Initial, Boundary Conditions

Since this is a multi-region simulation, every region has been assigned different initial conditions based on its property.

Free Flow Region

In the *fluidDomain* region, free flow fluid is air. A free stream velocity is considered is Dirichlet condition, $u = u_\infty = 10m/s, v = w = 0$ is assigned to the inlet. Since there is consideration of evaporation from the porous region to the free stream region, initial mass fractions of *specieA* and *specieB* are set to 0, while initial mass fraction of air is kept at 1. The temperature of the region is constant at 450K in the beginning. The initial conditions for *fluidDomain* are given in table 5.5.

Boundary	type	Value
Inlet	Velocity	$u_x = 10m/s, v = w = 0$
Outlet	Pressure	1e5
air	mass fraction	1
specieA	mass fraction	0
specieB	mass fraction	0

TABLE 5.5: Initial and boundary conditions for *fluidDomain*

Heater

Heater is supposed to be solid. There is solid-fluid coupling between the fluid and heater regions as well as between the heater and porous regions. This coupling from heater-fluid can be given in OpenFoam, as shown in figure 5.7. The initial temperature of the heater is supposed to be 450K.

```
heater_to_fluidDomain
{
    type            compressible::turbulentTemperatureCoupledBaffleMixed;
    Tnbr           T;
    kappaMethod    solidThermo;
    value          uniform 450;
}
```

FIGURE 5.7: Openfoam Coupling between Solid and Fluid Regions

The property of the heater is given in table 5.6. However, the material for the study is chosen to be artificial and cannot be used for some real-life problems.

Properties	Value
Density	$8400 [Kg/m^3]$
Thermal Conductivity	$13.4 [W/(m * K)]$
Molecular Weight	50
Heating Power	$3 \times 10^8 [W]$
Heat capacity at constant Pressure	$440 [J/(kg * K)]$

TABLE 5.6: properties of the heater used for Simulation (arbitrary material)

Porous

It is supposed in the study that the porous medium is saturated with the arbitrary binary liquids *specieA* and *specieB*, and there is a continuous supply of the liquids to the porous region from a free liquid region. It means that during the evaporation from porous media, evaporation stage 1 is maintained during our study, as explained in chapter 4.1. Properties of *specieA* and *specieB* are given in table 5.7.

Due to the flow through porous media, flow of multiphase liquids is governed by porous properties. In the calculation of sink values in governing equation 5.1, it

Property	specieA	specieB
molecular weight	75	80
Heat capacity at constant Pressure	170 [J/(kg * K)]	220 [J/(kg * K)]
Coefficient of viscosity	0.04 [kg/(m * s)]	0.8 [kg/(m * s)]
Enthalpy of Vaporisation	62000 [J]	90000 [J]
Boiling Point	482 [K]	520 [K]

TABLE 5.7: Properties of Arbitrary liquids specieA and specieB

is required to have D and F coefficients. These coefficients are given for an arbitrary porous material:

$$D = (100 \ 0 \ 0) \quad (5.27)$$

$$F = (0 \ 0 \ 0) \quad (5.28)$$

5.6 Summary of the Chapter

In this chapter, we discussed the *OF* tools used in numerical simulations. We started our discussion with the description of the *OF* solver *porousEvapFoam*. We discussed in details about the momentum conservation equation used in the solver, its discretization into finite volume methods (FVM), the PIMPLE Algorithm and, then talked about the numerical schemes offered by the *OF*. In the end, we looked into the case setup for the simulation for the numerical study. The geometry contains three different regions, heater, free-flow and porous regions. We discussed the details of the initial and boundary conditions for each region.

In the next chapter, we will see the results of the numerical simulations.

Chapter 6

Results and Discussions

The setup of the test case taken for this study is already explained in chapter 5.5. The simulation is done using OpenFOAM v9, and *ParaView* is used to visualise and post-process the results obtained from the simulation. In this chapter, we have discussed the results from the transient simulation of the evaporation effects from porous media.

Two cases have been simulated to study the effect of porous media on the evaporation of liquids to the free flow. They are:

- Case 1: In this case, the saturated porous media is taken into the consideration. All effects of porous media is also considered. Due to drying from interface to the free-flow region, it is expected to have creeping flow of liquids within the porous media towards the interface from the multi-species liquid reservoirs.
- Case 2: In this case, we considered that no porous media is present and multi-species liquid has a sharp interface with the free flow and heater. Since liquid is evaporated at the interface, there is no induced flow within the liquid phase. It is expected to have high evaporation rate.

6.1 Porous Media Effect on Evaporation

In this section, we will talk about the results of the effects of the porous medium on the start of evaporation of different phases, rate of evaporation of different phases, and rate of change of boiling points of the mixtures.

Simulation results about the evaporation are shown in figure 6.1 and 6.2.

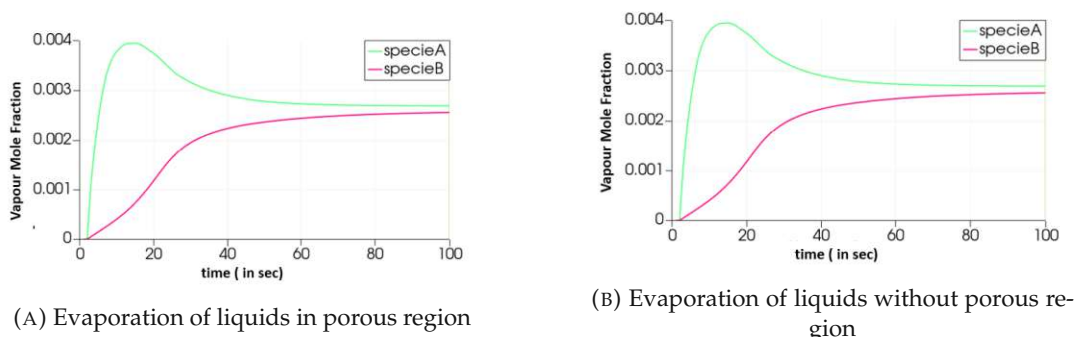


FIGURE 6.1: Comparison of the beginning of evaporation of two cases

In the considered mixtures of liquids *specieA* and *specieB*, *specieB* has a higher boiling point and enthalpy of evaporation than *specieA*. Due to the lower boiling

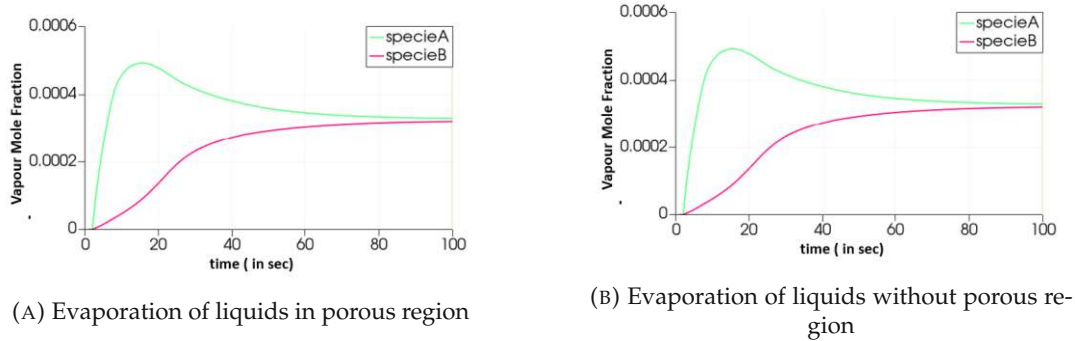


FIGURE 6.2: Comparison of evaporation of liquids at the outlet

point, it is obvious that specieA started to evaporate earlier than specieB in both cases. But when the temperature of the system reached higher than the boiling point of both components, the rate of evaporation of the mixture increased instead of just a single phase.

As shown in the results, there is no effect of a porous media flow on the beginning of the liquid's evaporation. It can be explained that the porous media is fully saturated with multi-species liquids. Hence, in the beginning, no porous media resistance acted, and the beginning of evaporation is the same for both cases. Later, due to porous resistance, the vapour fractions in free stream reduced than without porous medium. Figure 6.1 compares the vapour flux of different components after evaporation in porous media to the free stream region at the porous medium-free stream interface. Figure 6.2 compares the vapour flux of specieA and specieB at the outlet of the free flow region.

6.2 Porous Media Flow Results

Due to evaporation from porous media to the free flow region, there is an induced flow regime within the porous medium. This induced flow regime has been generated due to the capillary action of the porous medium. Capillary action worked as a pressure gradient to guide the liquids to the drying front. The speed of fluid flow depends on the rate of evaporation, porous media properties and fluid viscosity. Hence, in this case, the speed of fluid flow depends mainly on the rate of the evaporation at the drying front to the free flow region.

The figure 6.3 shows the streamlines of the flow within the porous medium. Before time $t = 2s$, there was no velocity field within the porous region. At time $t = 2s$, when evaporation of the specieA started, the velocity field was produced due to the movement of liquids, but the velocity was very slow ($\approx 10^{-6} m/s$). As soon as specieB also started to evaporate, the velocity within the porous region increased rapidly (of an order of $\approx 10^{-3} m/s$). After $t = 30s$, the system reaches towards equilibrium and at that the flow velocity with porous medium is highest at $1.8 \times 10^{-3} m/s$. The streamlines stabilized afterwards, showing that the system reached an equilibrium condition.

Figure 6.4 shows the distribution of the specieA and specieB at different intervals in the porous region. Due to the lower boiling point and enthalpy of evaporation

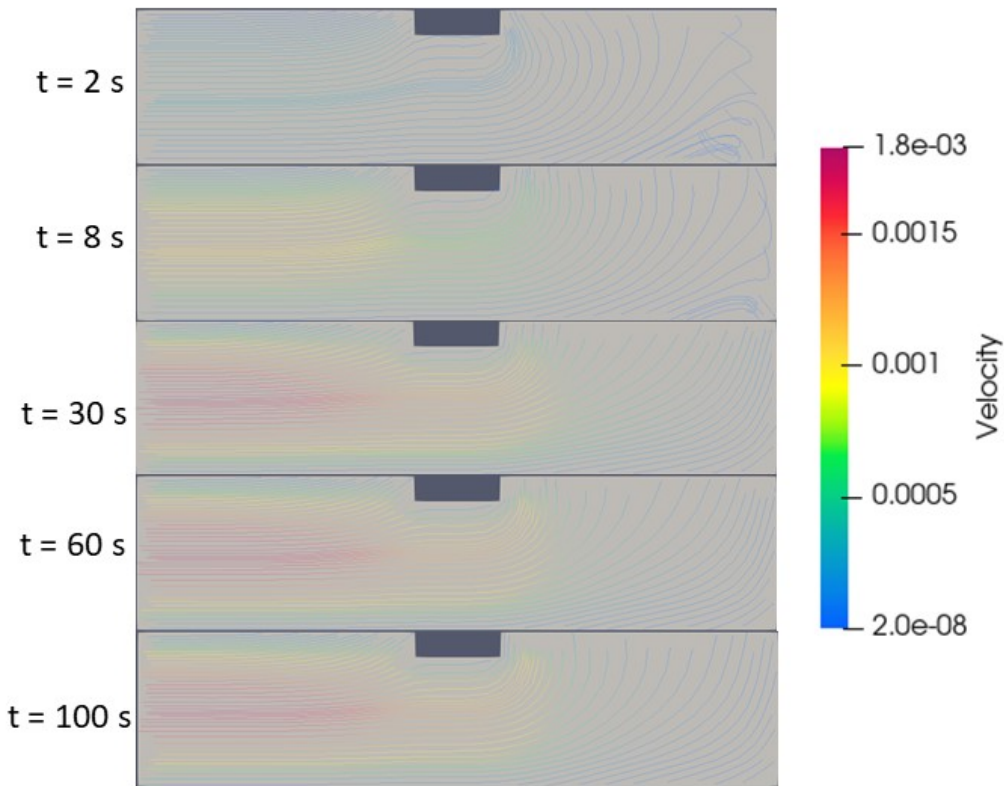


FIGURE 6.3: Flow of multi-species liquids within porous media towards drying front at different time

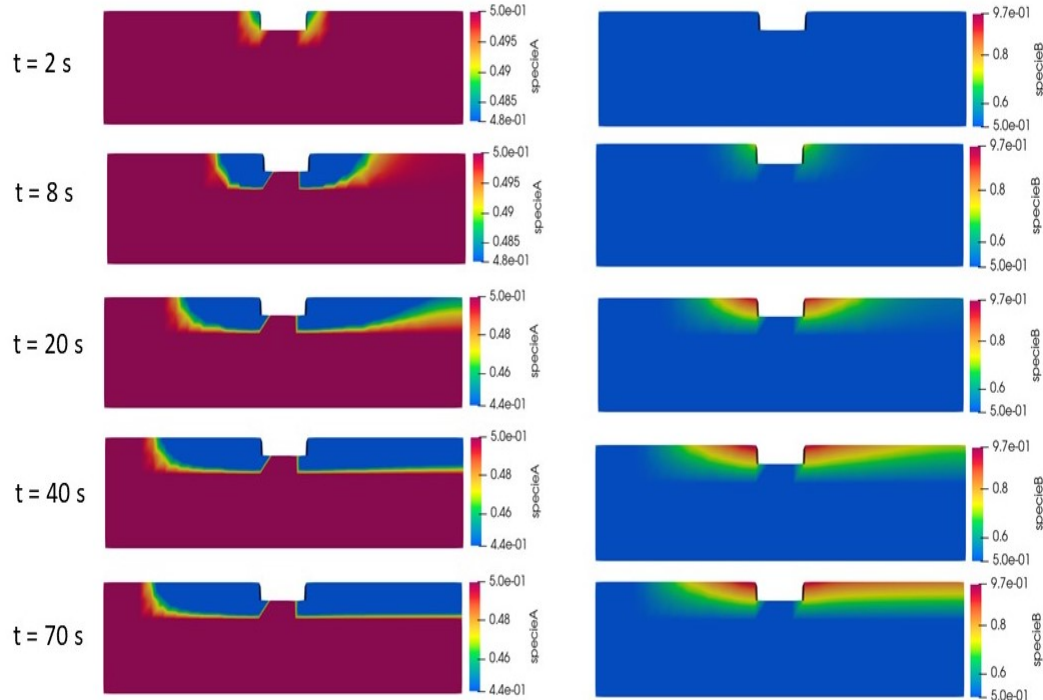


FIGURE 6.4: Proportion of liquid species in the porous media at different intervals due to drying from porous media

of specieA, it started to evaporate earlier than specieB at $t = 2\text{s}$ near the heater region. Due to this, the proportion of the specieB in such region increased enormously. When the temperature of the mixture reached above the boiling point of the specieB, it started to evaporate at $t = 8\text{s}$. But, still, the rate of evaporation of the specieA dominated the specieB.

6.3 Temperature Effect on Evaporation

Due to heating through the heater, the temperature of the system increased. To have an understanding of the temperature field in the free flow region, we plotted a graph at a point near the heater in the free flow region. The graph showed the evolution of the temperature field with time at that point. The graph can be seen in figure 6.5.

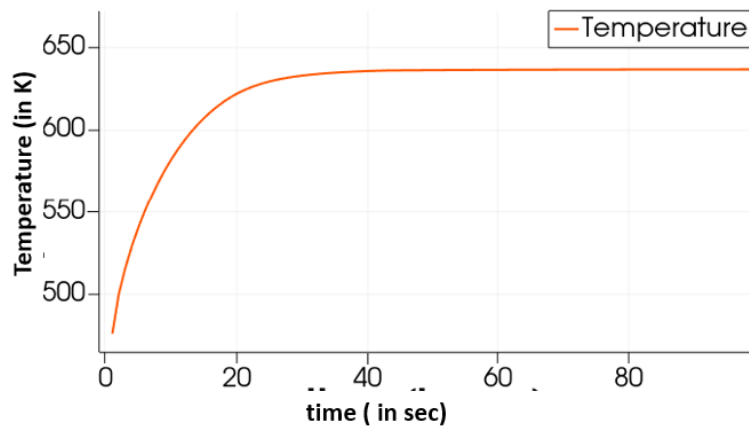


FIGURE 6.5: Evolution of the temperature in the free-flow regime at a point near the heater

It can be seen in figure 6.5 that the temperature field in the free flow region stabilized after $t = 30\text{s}$, even though the heater continued to heat. It can be explained in the term that the energy provided by the heater is utilized by the multi-component's liquid phase to change its phase to gaseous, and also the maintaining the temperature field constant in the whole domain as fluid entered the domain at 450K only.

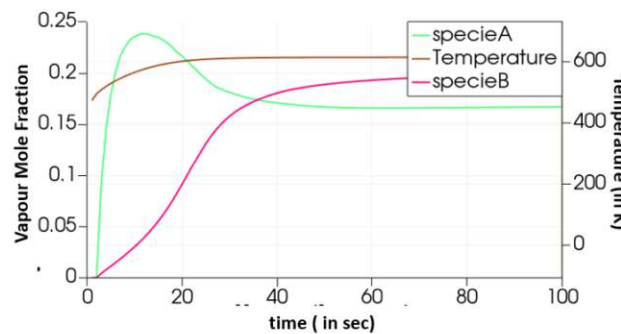


FIGURE 6.6: Variations of the proportion of each component with temperature

Figure 6.6 presents a plot between proportions of different components with the temperature. In the beginning when the temperature in the field was above the boiling point of the specieA, the rate of evaporation was high for specieA. But, as the temperature field reached above the boiling point of the specieB, the rate of evaporation of the specieA reduced and evaporation rate for the specieB peaked. It can be explained as when the temperature is above the boiling point of specieA; the rate of evaporation is high near the heater. Due to this, the proportion of specieB near the heater reached a lot higher than specieA. As soon as the temperature field reached above the boiling point of specieB, it started evaporating, absorbing the enthalpy of evaporation, due to which the rate of evaporation of specieB went up and vice-versa for specieA.

6.4 Evaporation Effect on Free Flow

The Effect of evaporation from porous media can be observed in the free-flow region through the measurement of the proportions of each component. As predicted, as the proportion of the evaporated liquids went up in the free-flow region, the proportion of air in the vicinity of the porous region went down. In figures 6.7, 6.8, and 6.9, we can see the variations along the length of the free flow region at different time intervals.

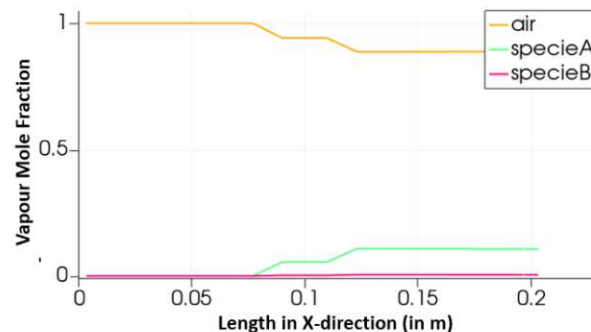
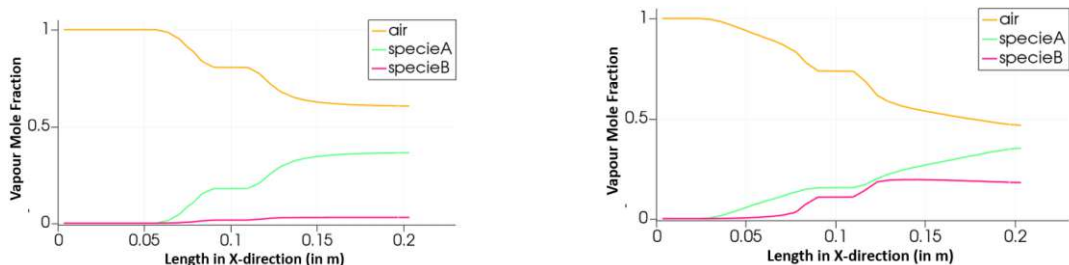


FIGURE 6.7: Proportion of each component in the gaseous region at $t = 3s$



(A) Proportion of each component in the gaseous region at $t = 8s$

(B) Proportion of each component in the gaseous region at $t = 30s$

FIGURE 6.8: Proportion of each component in the gaseous region at $t = 8s$ and $t = 30s$

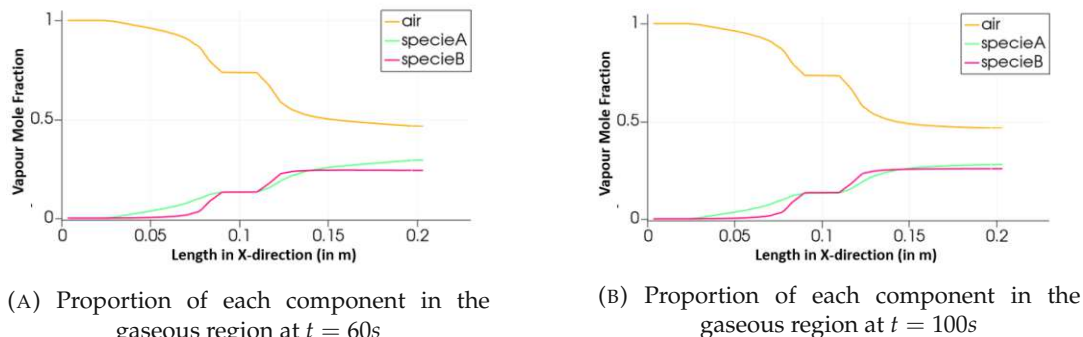


FIGURE 6.9: Proportion of each component in the gaseous region at $t = 60\text{ s}$ and $t = 100\text{ s}$

At time $t = 3\text{ s}$, the specieA started to evaporate and diffuse into the free flow stream. But, specieB haven't been evaporated yet. At time $t = 8\text{ s}$, evaporation of specieB just started and start to diffuse into the free flow region. After time $t = 30\text{ s}$, the flow regime started to move towards equilibrium. It can be realized in the figure 6.9b. The proportions of each component started to stabilize in the free flow region. The same results can also be realized in figure 6.10.

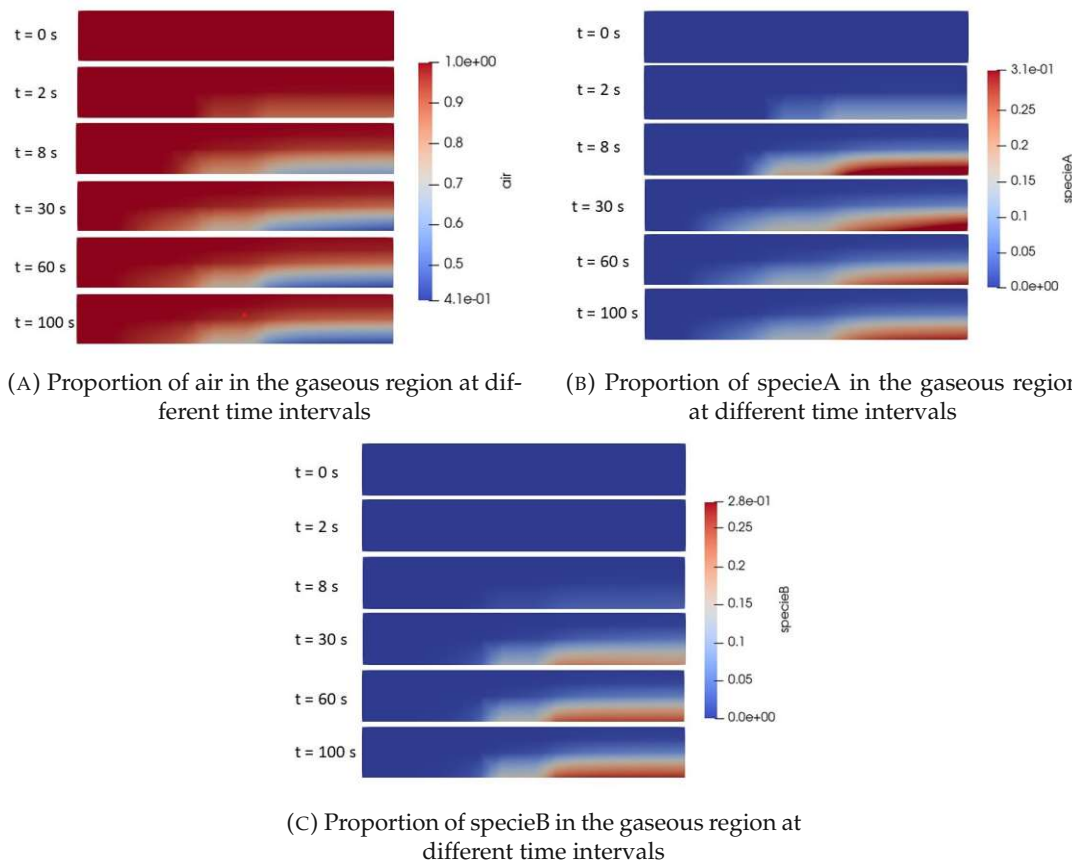


FIGURE 6.10: Proportions of each components at different time intervals

6.5 Multiprocessor Simulation Results

we ran the case simulation over several processors to get the best number of processors to decompose the domain into. Simulation was performed using *AMD EPYC 7453* CPU. The simulation was done on 1, 2, 4 and 8 cores and compared their run time. Table 6.1 shows the run time results on the different numbers of cells.

Number of cores	Run time (in s)
1	4890
2	2030
4	3116
8	3198

TABLE 6.1: The run time of simulation with several numbers of cores

The plot between run time and the number of cores is shown in figure 6.11:

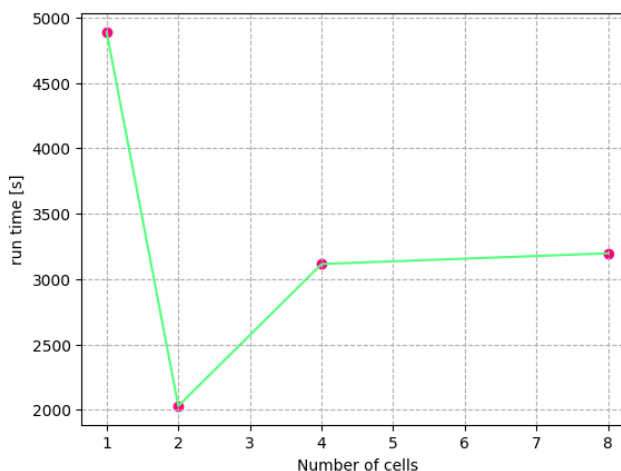


FIGURE 6.11: Runtime of simulation on various no. of processors

In figure 6.11, we can observe that when no of processors is increased from 1 to 2, then simulation computation time is halved. However, when these numbers are increased from 2 to 4, the run time increases sharply. Hence, the simulation on 2 number of the processor is most computationally effective in the present study. It can be explained in the term that since the number of cells in the computational domain are not enough (3000 total cells), the fraction of cells to each processor is reduced when more processors are there. In such cases, processors spent more time communicating with other processors than doing computations, which can be observed with the number of processors 4 and 8.

6.6 Computation Time Comparison

To study the effects of the number of cells on the run time during the simulation, we simulated over different numbers of cells. We ran the simulation over 3000, 6000, 12000, and 24000 cells. The simulation was performed using 2 number of cores as we get the best run time. The run times have been given in table 6.2.

Here, we observe the linear relationship between number of cells and computation time. This is due to the fact that the meshes are simple blocks. For a complex

Number of cells	Run time (in s)
3000	2030
6000	3507
12000	6085
24000	10178

TABLE 6.2: The run time of simulation with various number of Cells
on 2 processors

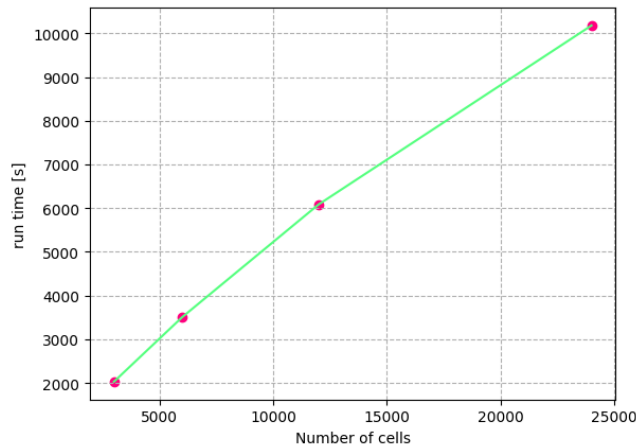


FIGURE 6.12: Curve for the run time vs. number of cells

geometry, the computation time had shown exponential increment concerning the number of cells.

Chapter 7

Conclusions and Future Work

The effects of various parameters on the evaporation of the multi-species liquids have been studied in this work to develop a better understanding of the rate of evaporation from a porous media. Numerous numerical simulations have been performed with varying parameters to evaluate the evaporation rate. Only stage 1 drying is considered in this study. The following conclusions were extracted based on the present work:

- The liquid front directly exposed to the free flow has a higher evaporation rate than the porous media saturated with the liquids as expected.
- In evaporation from the porous media, there is induced creeping flow within the porous media interior. This induced creeping flow is generated due to the effect of the capillary action.
- Free flow velocity was found to have a profound impact on the rate of evaporation. When velocity in free flow region is high, the rate of evaporation is higher. It can be explained as rate of evaporation is based on the saturation pressure and partial pressure of the liquid components in the surroundings. The higher velocity of free flow reduced the partial pressures of evaporating components.
- The temperature of the system played an integral role in the evaporation. When temperature of the system has been raised above the boiling point of the one constituent of the multi-species liquid, the respective constituent started to evaporate, due to which the proportion of the other component raised high in the vicinity of the interface.

Future Work Recommendations:

Following recommendations can be explored in the future works:

- Better understanding of the stage-2 drying and also the transition between stage 1 and stage 2.
- Implementation of two-domain coupling methods to improve the accuracy of the simulation.
- Looking for ways to characterize the porosity of the porous material at REV scale.
- Extend *porousEvapFoam* solver to work with convective evaporation from porous media.

Bibliography

- [1] Darcyforchheimer - openfoamwiki. <https://openfoamwiki.net/index.php/DarcyForchheimer>. (Accessed on 10/24/2022).
- [2] J. Bear. *Dynamics of fluids in porous media*. Courier Corporation, 1988.
- [3] A. Bouddour, J.-L. Auriault, M. Mhamdi-Alaoui, and J.-F. Bloch. Heat and mass transfer in wet porous media in presence of evaporation—condensation. *International Journal of Heat and Mass Transfer*, 41(15):2263–2277, 1998.
- [4] H. C. Brinkman. A calculation of the viscous force exerted by a flowing fluid on a dense swarm of particles. *Flow, Turbulence and Combustion*, 1(1):27–34, 1949.
- [5] H. Burcharth and O. Andersen. On the one-dimensional steady and unsteady porous flow equations. *Coastal engineering*, 24(3-4):233–257, 1995.
- [6] P. C. Carman. Fluid flow through granular beds. *Chemical Engineering Research and Design*, 75:S32–S48, 1997.
- [7] P. Chakraborty. *Evaporative drying from hydrophilic and hydrophobic single pores and porous media*. PhD thesis, 2022.
- [8] H. Class. *Multiphase flow and transport in porous media theory and modeling*. PhD thesis, Universität Stuttgart, Institut für Wasserbau, 2009.
- [9] H. Darcy. *Les fontaines publiques de la ville de Dijon: exposition et application...* Victor Dalmont, 1856.
- [10] M. K. Das, P. P. Mukherjee, and K. Muralidhar. *Modeling transport phenomena in porous media with applications*, volume 123. Springer, 2018.
- [11] P. Forchheimer. Wasserbewegung durch boden. *Z. Ver. Deutsch, Ing.*, 45:1782–1788, 1901.
- [12] W. G. Gray. A derivation of the equations for multi-phase transport. *Chemical Engineering Science*, 30(2):229–233, 1975.
- [13] K. R. Hall, G. M. Smith, and D. J. Turcke. Comparison of oscillatory and stationary flow through porous media. *Coastal engineering*, 24(3-4):217–232, 1995.
- [14] Z. Heinemann and G. Mittermeir. Fluid flow in porous media. 2013.
- [15] O. Hougen, H. McCauley, and W. Marshall. Limitations of diffusion equations in drying. *Trans. AIChE*, 36(2):183–206, 1940.
- [16] C.-T. Hsu and P. Cheng. Thermal dispersion in a porous medium. *International Journal of Heat and Mass Transfer*, 33(8):1587–1597, 1990.
- [17] M. Ilic and I. Turner. Convective drying of a consolidated slab of wet porous material. *International Journal of Heat and Mass Transfer*, 32(12):2351–2362, 1989.

- [18] V. Jambhekar, R. Helmig, N. Schröder, and N. Shokri. Free-flow–porous-media coupling for evaporation-driven transport and precipitation of salt in soil. *Transport in Porous Media*, 110(2):251–280, 2015.
- [19] D. Jamet, M. Chandesris, and B. Goyeau. On the equivalence of the discontinuous one-and two-domain approaches for the modeling of transport phenomena at a fluid/porous interface. *Transport in porous media*, 78(3):403–418, 2009.
- [20] B. B. Kazemian, Q. Guo, and P. Cheng. Direct numerical simulations of moisture transport in porous media by a multi-component/phase-change lattice boltzmann method. *International Journal of Heat and Mass Transfer*, 176:121264, 2021.
- [21] A. Kharaghani. *Drying and wetting of capillary porous materials: insights from imaging and physics-based modeling*. PhD thesis, Habilitationsschrift, Magdeburg, Otto-von-Guericke-Universität Magdeburg, 2020, 2020.
- [22] C. Kittel. *Elementary statistical physics*. Courier Corporation, 1958.
- [23] M. Knudsen. Maximum rate of evaporation of mercury. *Ann. phys.*, 47:697, 1915.
- [24] M. Knudsen. *The kinetic theory of gases, 3rd ed.* New York: Jon Wiley & Sons, 1950.
- [25] D. Koutsoyiannis. Clausius–clapeyron equation and saturation vapour pressure: simple theory reconciled with practice. *European Journal of physics*, 33(2):295, 2012.
- [26] Y. Le Bray and M. Prat. Three-dimensional pore network simulation of drying in capillary porous media. *International journal of heat and mass transfer*, 42(22):4207–4224, 1999.
- [27] P. Lehmann and D. Or. Evaporation and capillary coupling across vertical textural contrasts in porous media. *Physical Review E*, 80(4):046318, 2009.
- [28] W. K. Lewis. The rate of drying of solid materials. *Industrial & Engineering Chemistry*, 13(5):427–432, 1921.
- [29] K. Mosthaf, R. Helmig, and D. Or. Modeling and analysis of evaporation processes from porous media on the rev scale. *Water Resources Research*, 50(2):1059–1079, 2014.
- [30] D. Nield. Modelling fluid flow in saturated porous media and at interfaces. In *Transport phenomena in porous media II*, pages 1–19. Elsevier, 2002.
- [31] J. Raju. *Multi-phase interface area calculation using Iso-Alpha method*. PhD thesis, Wien, 2020.
- [32] O. Reynolds. *The sub-mechanics of the universe*, volume 3. University Press, 1903.
- [33] L. A. Richards. Capillary conduction of liquids through porous mediums. *Physics*, 1(5):318–333, 1931.
- [34] A. E. Scheidegger. The physics of flow through porous media. In *The Physics of Flow Through Porous Media (3rd Edition)*. University of Toronto press, 2020.

- [35] T. Shaw. Drying as an immiscible displacement process with fluid counterflow. *Physical Review Letters*, 59(15):1671, 1987.
- [36] T. K. Sherwood. The drying of solids—i. *Industrial & Engineering Chemistry*, 21(1):12–16, 1929.
- [37] K. Vafai and C. L. Tien. Boundary and inertia effects on flow and heat transfer in porous media. *International Journal of Heat and Mass Transfer*, 24(2):195–203, 1981.
- [38] W. B. Van Arsdel. Approximate diffusion calculations for the falling-rate phase of drying. 1947.
- [39] S. Whitaker et al. Coupled transport in multiphase systems: a theory of drying. *Advances in heat transfer*, 31:1–104, 1998.
- [40] C. Wu, T. Zhang, J. Fu, X. Liu, and B. Shen. Random pore structure and rev scale flow analysis of engine particulate filter based on lbm. *Open Physics*, 18(1):881–896, 2020.
- [41] Z. Zhang, S. Yang, and D. Liu. Mechanism and mathematical model of heat and mass transfer during convective drying of porous materials. *Heat Transfer—Asian Research: Co-sponsored by the Society of Chemical Engineers of Japan and the Heat Transfer Division of ASME*, 28(5):337–351, 1999.